FRM II
Forschungs-Neutronenquelle
Heinz Maier-Leibnitz

MLZ
Heinz Maier-Leibnitz Zentrum

(Magnetic) Small Angle Neutron Scattering Theory, Instrumentation and Applications

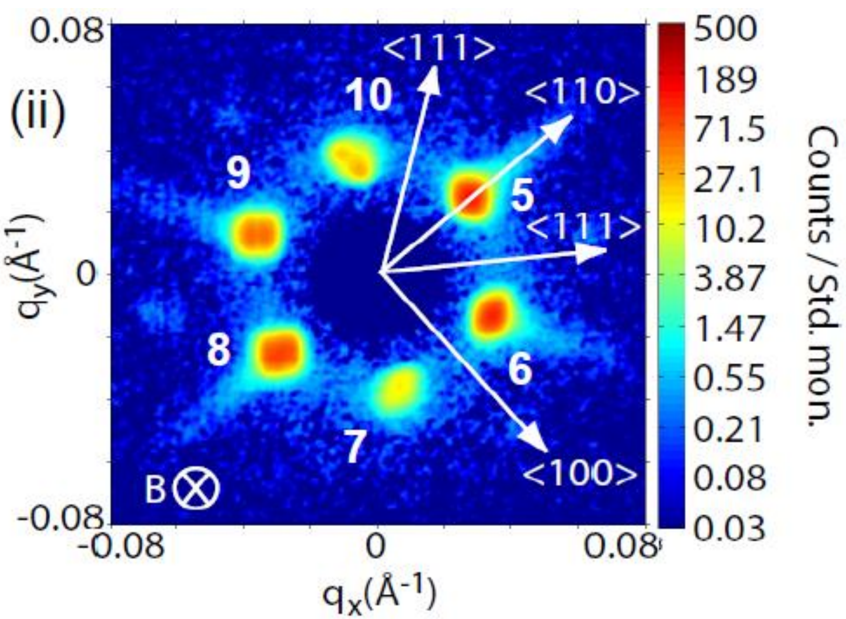

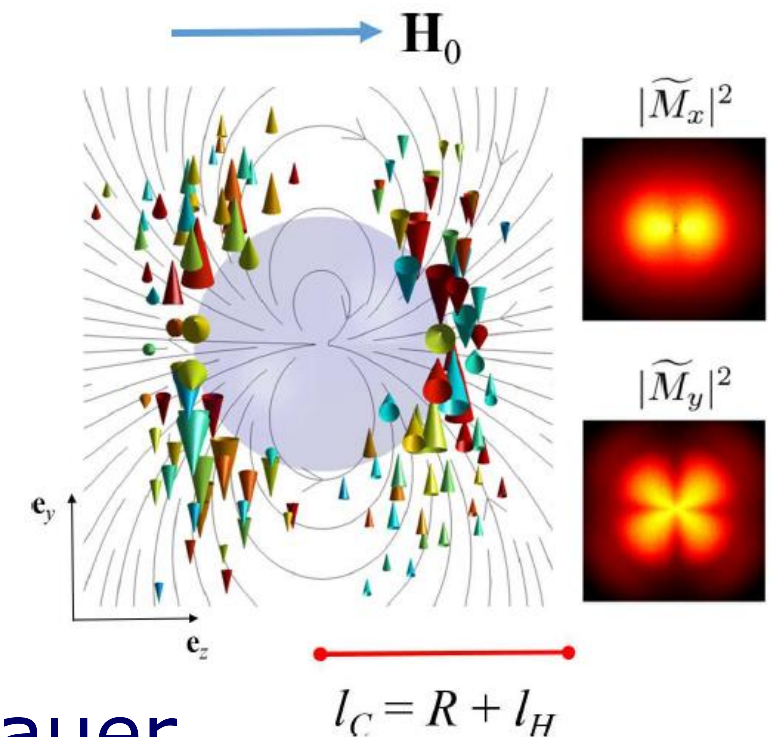

S. Mühlbauer

Czech-Bavarian Mini School, 19.10.2020

Acknowledgments

Research at large scale facilities: A team effort!

P. Böni	*SCES TUM*
C. Pfleiderer	*E21/E51*
F. Jonietz	
T. Adams	
J. Kindervater	
T. Reimann	
A. Backs	
D. Mettus	
F. Haslbeck	
A. Rosch	*Köln*
M. Garst	*Karlsruhe*
B. Wolba	
A. Wilhelm	*FRM II*
S. Semecky	
M. Schulz	
K. Zeitelhack	
I. Defendi	
W. Petry	
U. Reinecke	
R. Gilles	
X. Brems	
M. Dembski-Villalta	

A. Heinemann	*HZG*
S. Busch	
A. Beldowski	
O. Listing	
D. Heims	
J. Borchers	
G. Musilak	
D. Siemers	
J. Hedde	
J. Hübscher	
S. Demirdis	*JCNS*
V. Pipich	
E. M. Forgan	*Birmingham*
A. Holmes	
E. Blackburn	
M. Laver	
H. Furukawa	*RIKEN*
M. Soda	
N. Kagamida	
U. Keiderling	*HZB*
R. Cubitt	*ILL*

Outline

SANS – Basic Concept & Theory

SANS – Instrumentation

SANS – Resolution & Intensity

Applications & Examples of SANS:

- Soft Matter
- Hard Matter
- Magnetism of nanoscale materials
- Emergent nanoscale magnetic structures of strongly correlated electron systems (SCES)

SANS – Basic Concepts

SANS: Diffractometer specialized for small scattering angles

Large correlations in real space 20Å to 40.000Å ⟺ Low **Q** small scattering angles ~1 $Å^{-1}$ to ~10^{-4} $Å^{-1}$

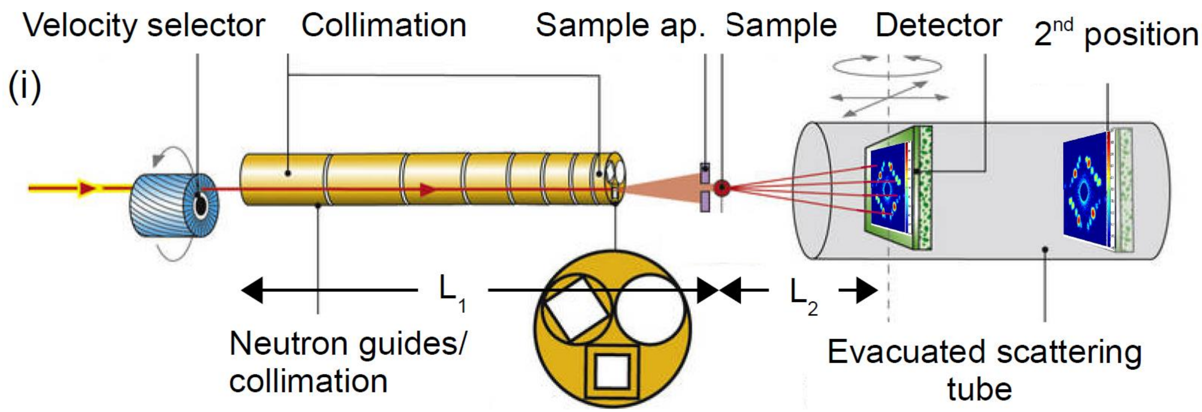

SANS-1 @ MLZ

A joint TUM/HZG project

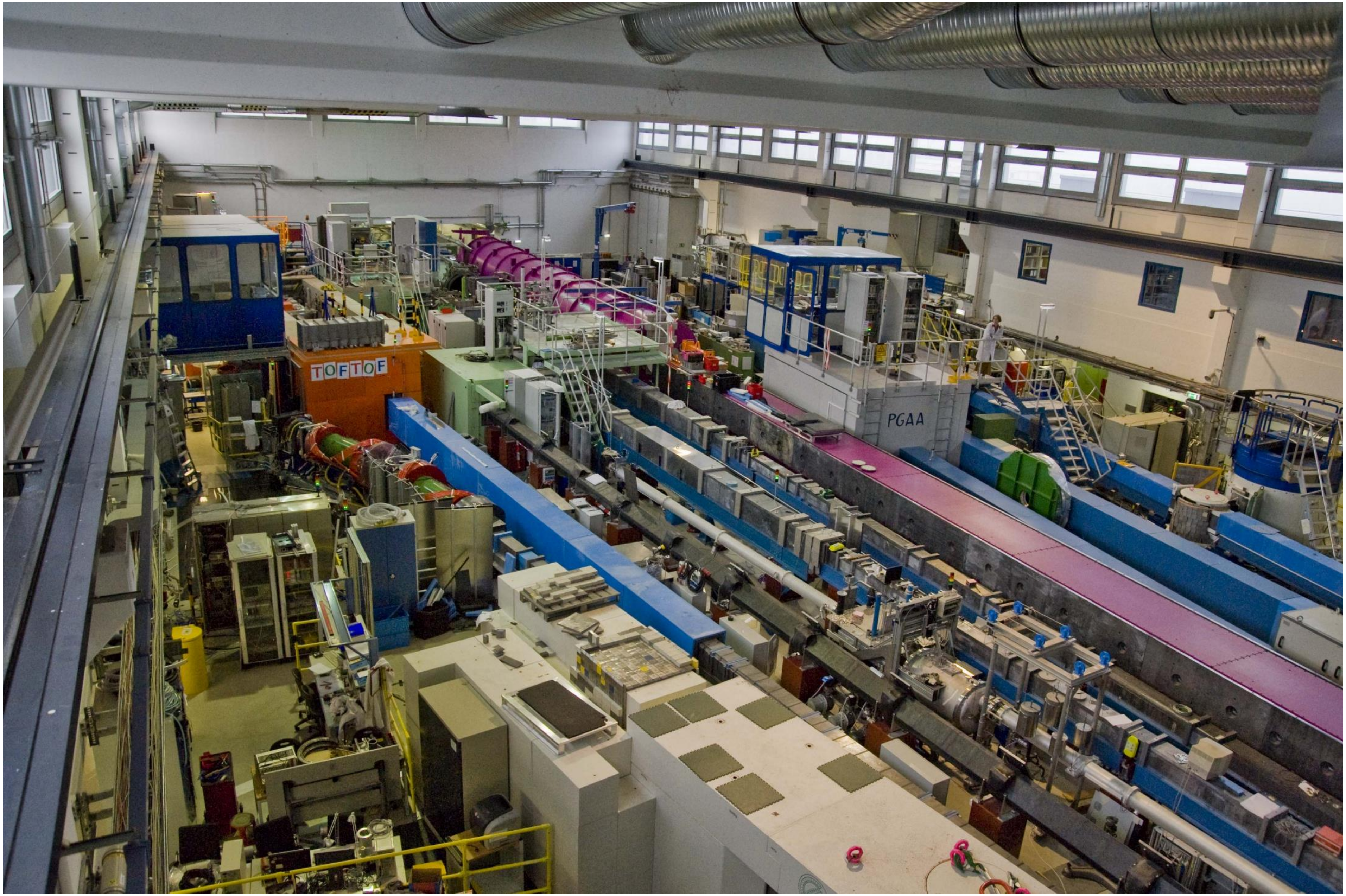

SANS vs. SAXS

Properties of neutrons

Interaction with the nuclei (*strong* interaction, pointlike)

Neutral particle, deep penetration (window materials for extreme environment)

Isotope sensitivity

No radiation damage to samples

Sensitive to magnetism (spin1/2 particle)

Energy and momentum match elementary excitations and interatomic distances of condensed matter

Low brilliance (many orders of magntitude compared to X-rays)

Brilliance cannot be scaled up easily

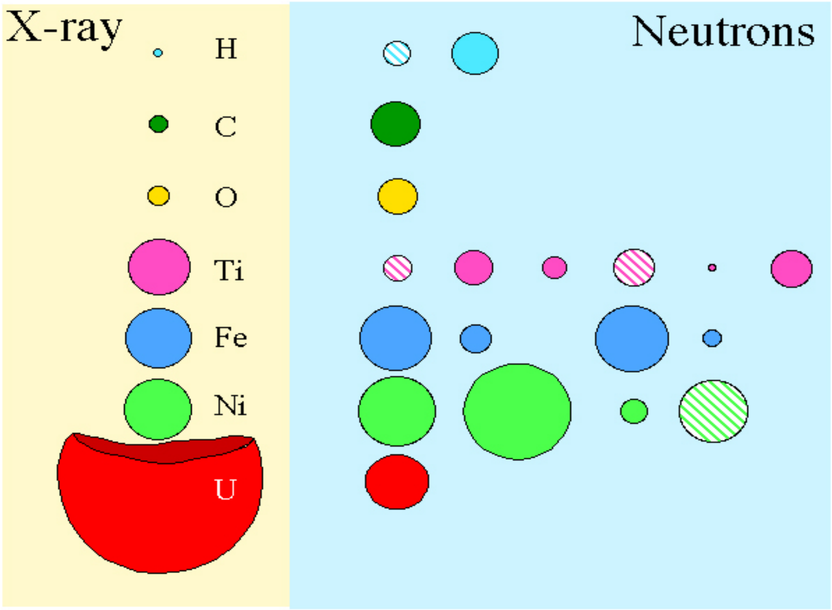

Table 1.2: Properties of the Neutron.

Physical quantity	Quantity	Dimension
Mass	$1.675 \cdot 10^{-27}$	kg
Charge	0	C
Spin	$1/2$	$\hbar$
magn. dipol moment	$\mu_n = -1.913\,\mu_K$	$\mu_K = \frac{e\hbar}{2M_pc}$
nuclear magneton		$1\,\mu_K = 0.505 \cdot 10^{-23}$ erg/G
		$1\,\mu_K = 3.15 \cdot 10^{-14}$ MeV/T
life time (free neutron)	886	s
kinetic energy	$E = \frac{1}{2}mv^2$	meV

Forward scattering - Why is it useful?

Backscattering Forward scattering

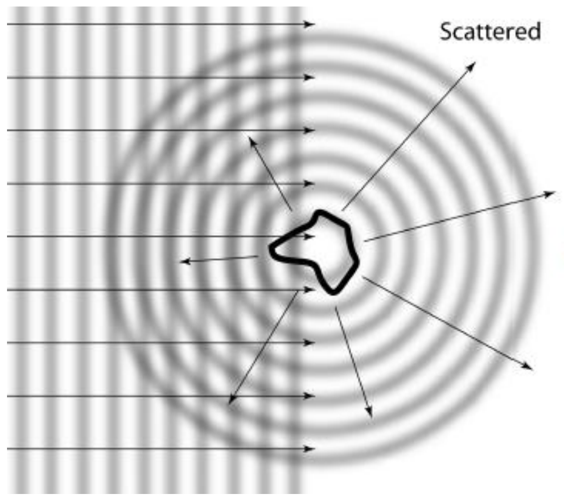

Phase function for different x

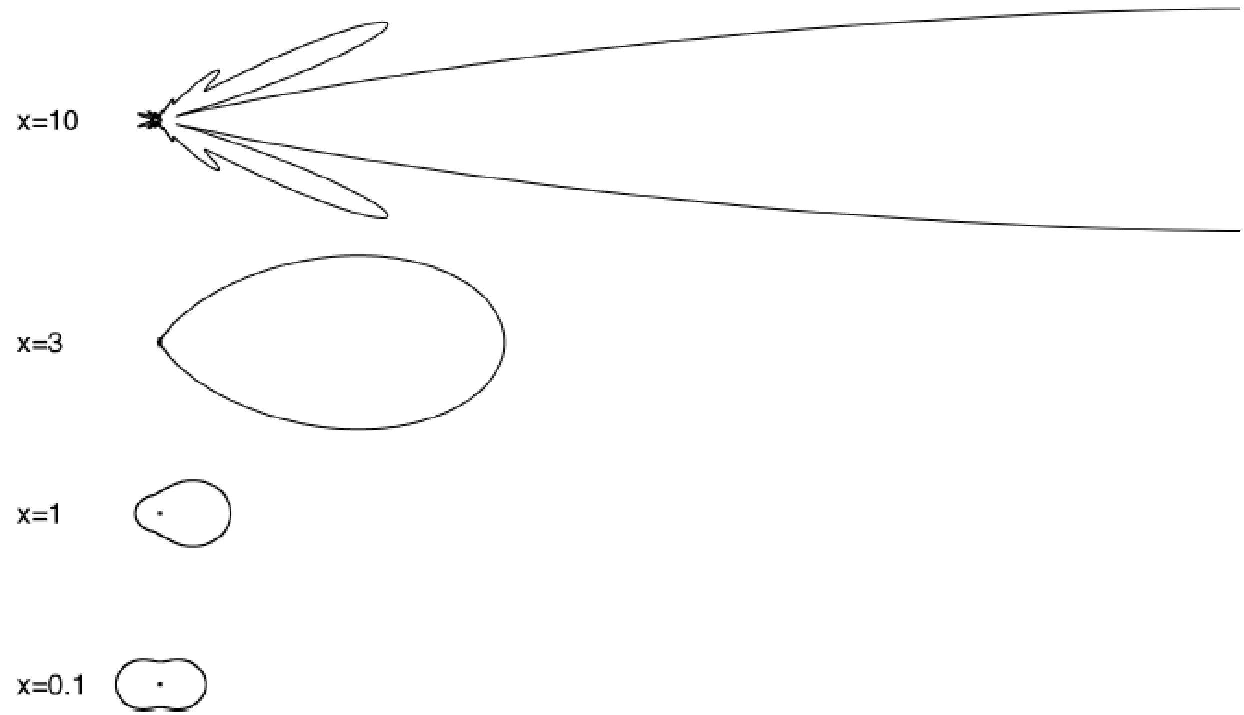

$$x = \frac{2\pi r}{\lambda}$$

⇨ Lots of intensity scattered in forward direction

Scattering length density

Neutron diffraction: Neutrons interact with individual nuclei with scattering length b

SANS: large structures/low q: Averages over large r

Scattering length b → Scattering length density

$$\rho = \frac{\sum_i^n b_i}{\overline{V}}$$

$$\rho(\mathbf{r}) = b_i \delta(\mathbf{r} - \mathbf{r_i})$$

Example: water

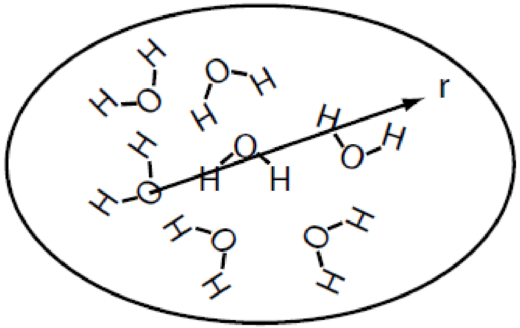

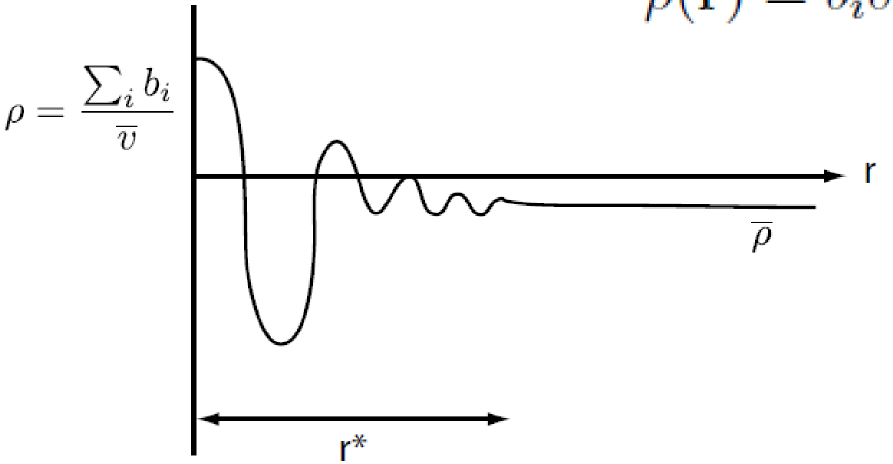

Scattering length density: Useful description for SANS, USANS, GISANS and reflectometry

Scattering length density: „Average interaction potential" for neutrons

Principle of Babinet

Assume a general two phase system

$$V = V_1 + V_2$$

$$\rho(r) = \begin{cases} \rho_1 & \text{in } V_1 \\ \rho_2 & \text{in } V_2 \end{cases}$$

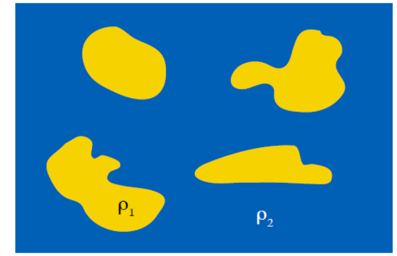

SANS measures inhomogeneities of scattering length density

$$\frac{d\Sigma}{d\Omega}(\mathbf{q}) = \frac{1}{V}(\rho_1 - \rho_2)^2 \left| \int_{V_1} e^{i\mathbf{q}\cdot\mathbf{r}} d\mathbf{r_1} \right|^2$$

Principle of Babinet: Same coherent scattering of these samples

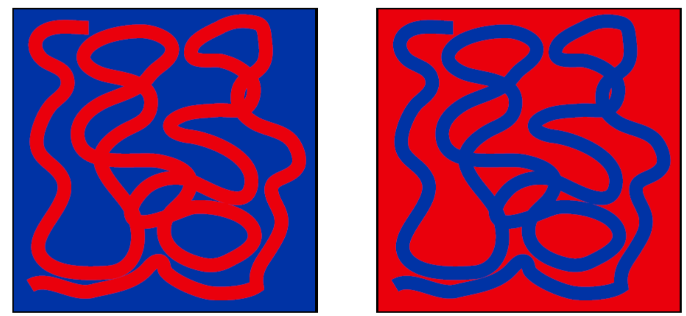

Contrast variation and contrast matching

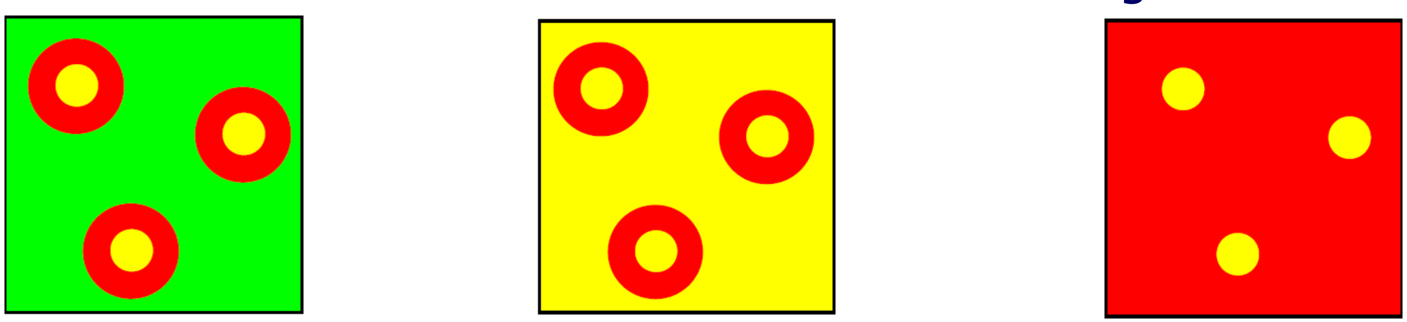

Natural contrast

Shell visible

Core visible

Mixture of H2O/D2O, isotope variation very useful for soft matter samples

Structure & Form Factor

$$\frac{d\Sigma}{d\Omega}(\mathbf{q}) = \frac{1}{V}(\rho_1 - \rho_2)^2 \left| \int_{V_1} e^{i\mathbf{q}\cdot\mathbf{r}} d\mathbf{r_1} \right|^2$$

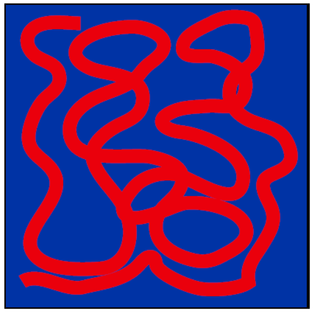

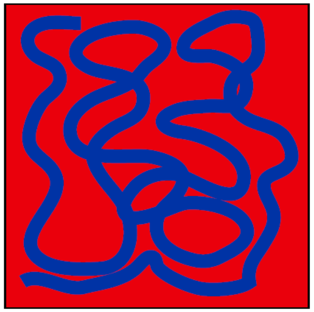

Split up the integral over the sample

$$\frac{d\Sigma}{d\Omega}(q) = \frac{N}{V}(\rho_1 - \rho_2)^2 V_p^2 P(q) S(q)$$

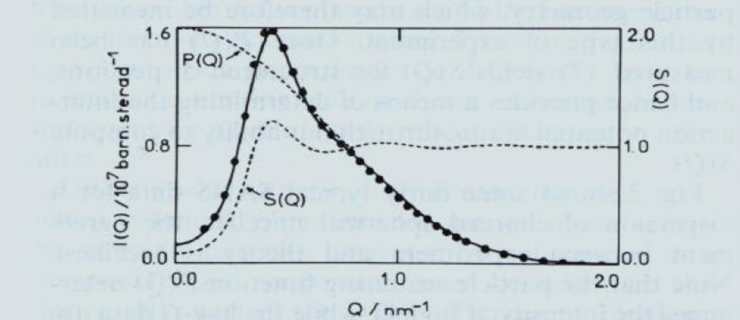

Fig. 2. Observed (●) and calculated (—) scattered intensity $I(Q)$ as a function of momentum transfer Q for a charged micellar dispersion: 0·03 mol dm^{-3} hexadecyltrimethylammonium chloride in D_2O at 313 K. The functions $P(Q)$ and $S(Q)$ are discussed in the text. (1 barn sterad^{-1} = 10^{-28} M^2 sterad^{-1}).

Form factor P(Q)

Interference of neutrons scattered at the same object

Shape, surface and densitiy distribution of objects

Structure factor S(Q)

Interference of neutrons scattered from different objects

Arrangement or superstructure of objects

Measurement signal:
Convolution of P(Q) and S(Q)

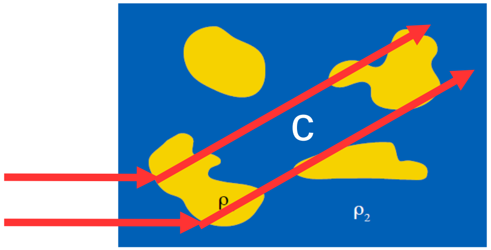

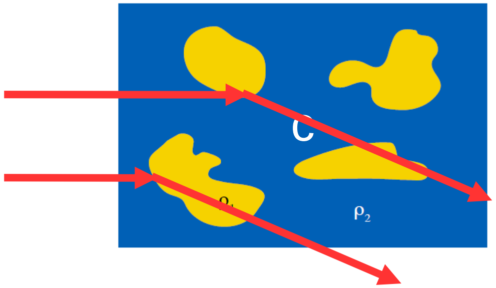

Form Factor

Lets assume a very diluted sample of randomly distributed identical scattering objects: No structure factor!

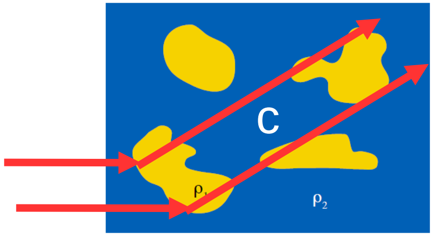

Form factor P(Q)

Interference of neutrons scattered at the same object

Patterson function:
Convolution of an object with itself

$$P(\mathbf{r}) = \int \rho(\mathbf{r}_1)\rho(\mathbf{r}_2)\, d\mathbf{V}, \qquad \text{with } \mathbf{r} = \mathbf{r}_1 - \mathbf{r}_2$$

Characteristic function (2D): Orientational average of P(r)

$$\gamma(r) = \frac{1}{2\pi}\int_0^{2\pi} P(\mathbf{r})\,\mathrm{d}\varphi$$

FT of Patterson function: Scattering signal

$$I(Q) = 4\pi \int_0^D \gamma(r)\frac{\sin(Qr)}{Q} r\,\mathrm{d}r$$

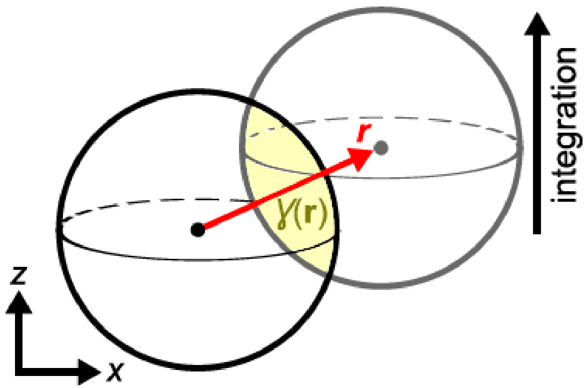

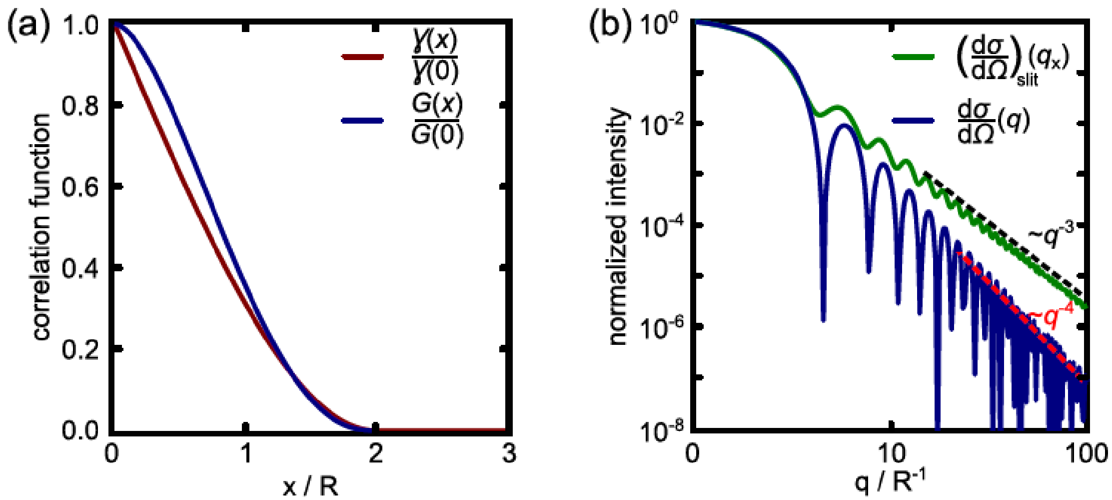

Form Factor

Diluted spheres

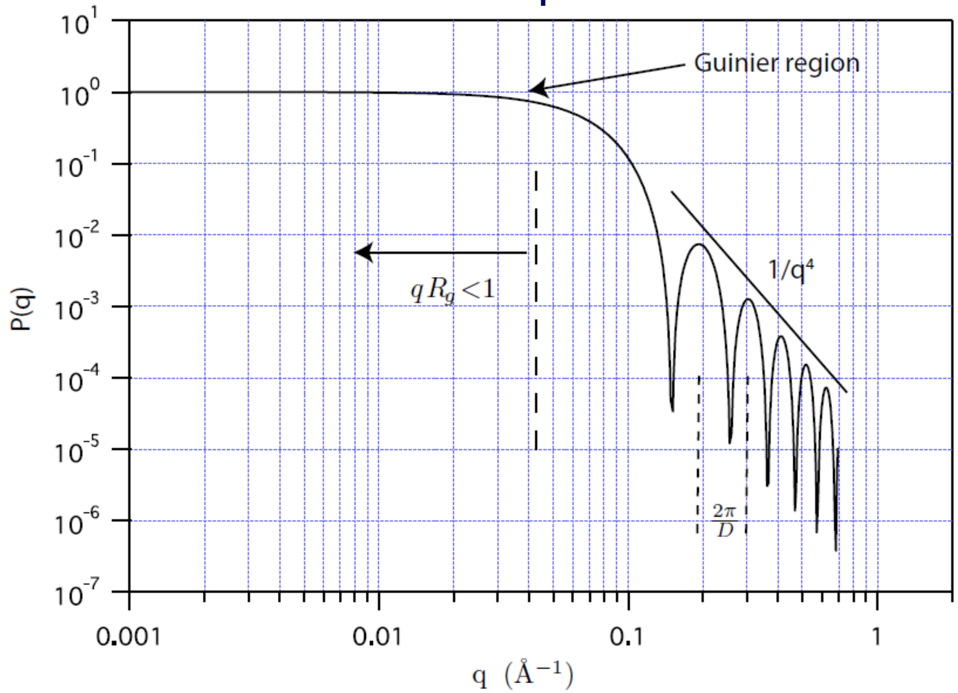

Random oriented diluted cylinders

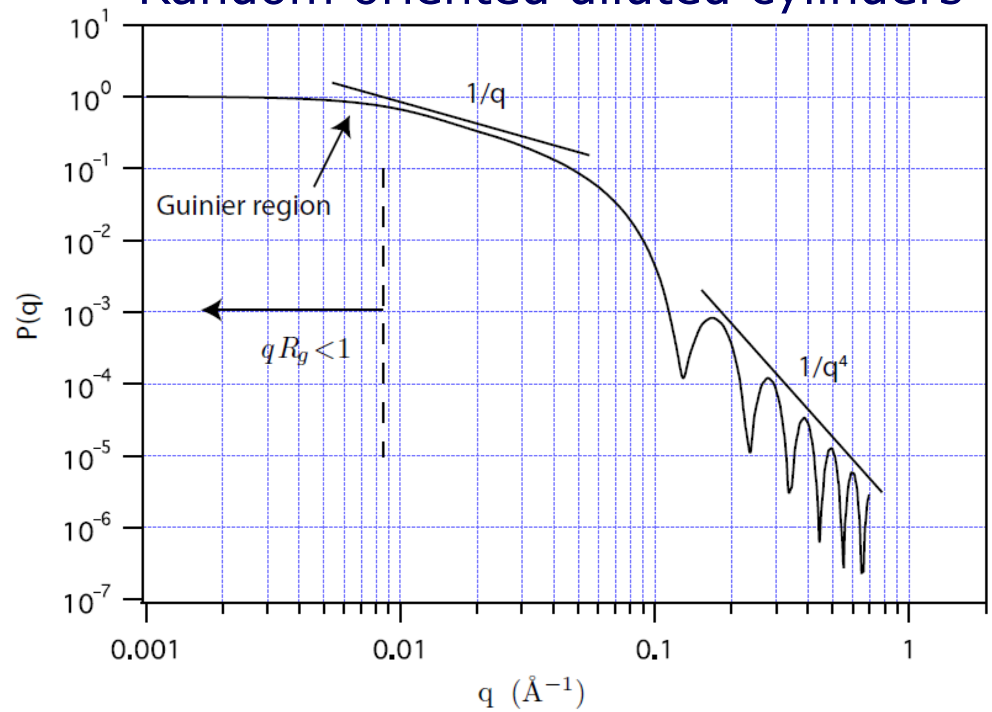

The form factor yields information about:
Shape, size (distribution), SLD contrast (profile)
and volume concentration of scattering objects.

But:
Prone to overfitting due to lack of independent parameters!

Form Factor

Low and high Q limits: Porod and Guinier regime

Form factor for diluted cylinders
radius 30Å, length 400Å
No structure factor!

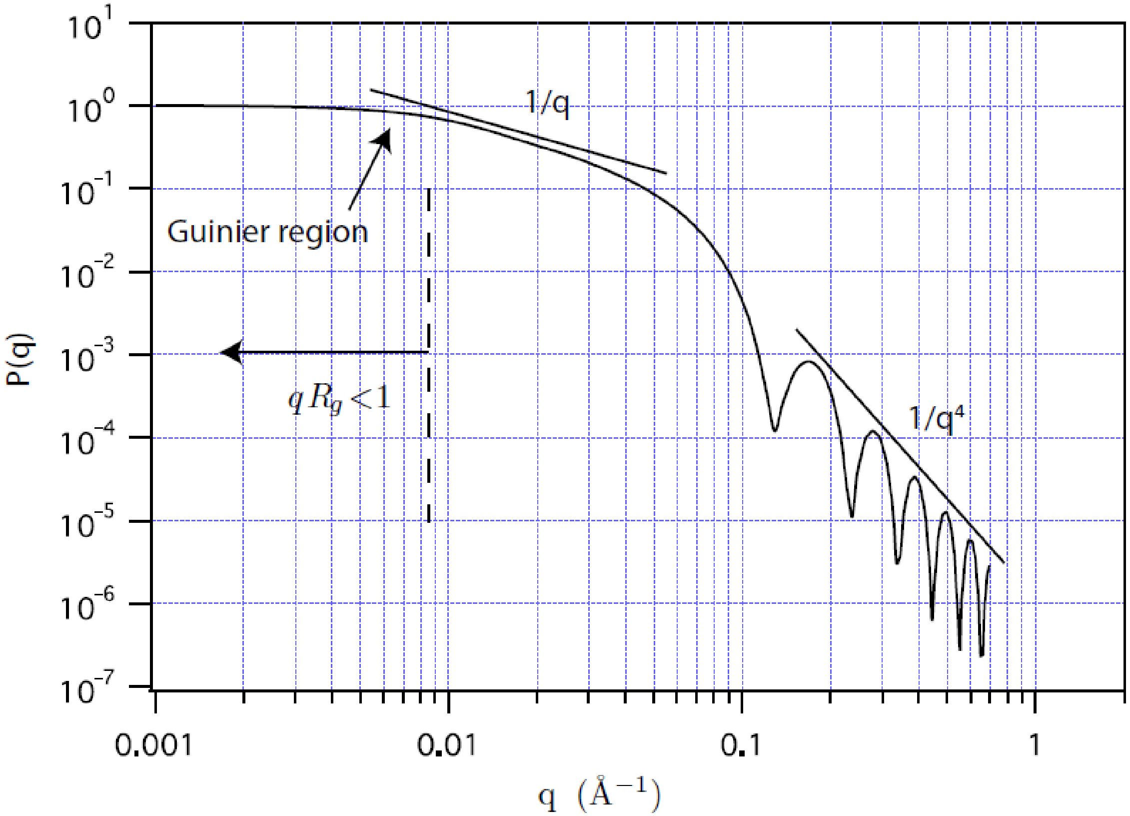

Porod scattering for smooth surfaces and $Q \gg 1/D$

$$I(q) \propto (q)^{-4}$$

$$\frac{\pi}{Q^\star} \cdot \lim_{q \to \infty} \left(I(q) \cdot q^4 \right) = \frac{S}{V}$$

Guinier scattering for dilute, monodisperse and isotropic solutions of particles:
$QR_G \ll 1$

$$I(q) = I(0) e^{\frac{-(qR_g)^2}{3}}$$

SANS: Instrumental Setup

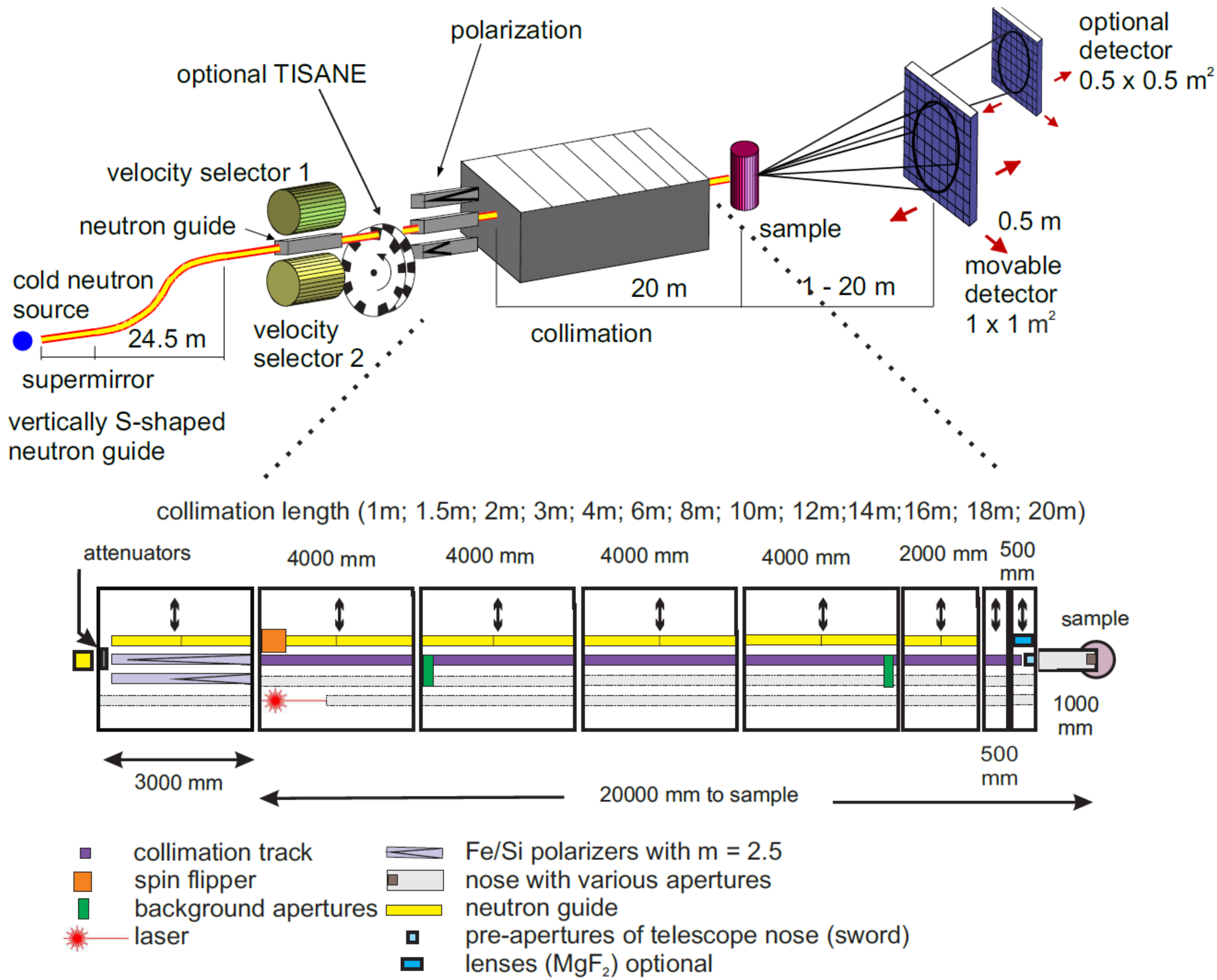

Collimation section

Velocity selector

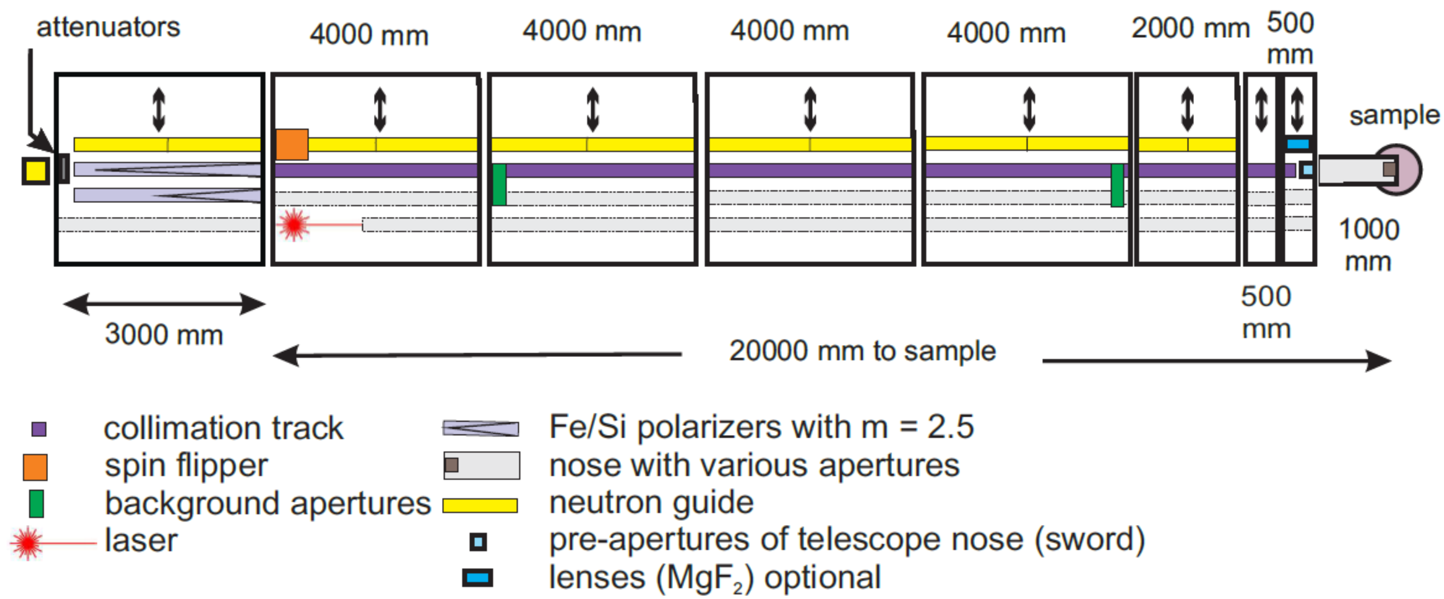

Collimation: Define resolution and intensity

Aperture system/neutron guides (supermirror)

Alignment extremely critical

Well-defined and homogenous wavelength /divergence profiles

Transmission polarizer for the use of polarized neutrons

Parasitic background scattering has to be avoided (whole collimation system is evacuated, edge scattering, incoherent background)

Sample stage

Provide necessary sample environment (similar to any other neutron diffractometer or spectrometer)

Parasitic background scattering has to be avoided (extremely critical!)

- Minimize neutrons travelling in air (few cm can be too much)
- Avoid Aluminum neutron windows (single crystalline sapphire is better)
- Get rid of scattering at edges (use conical slits)

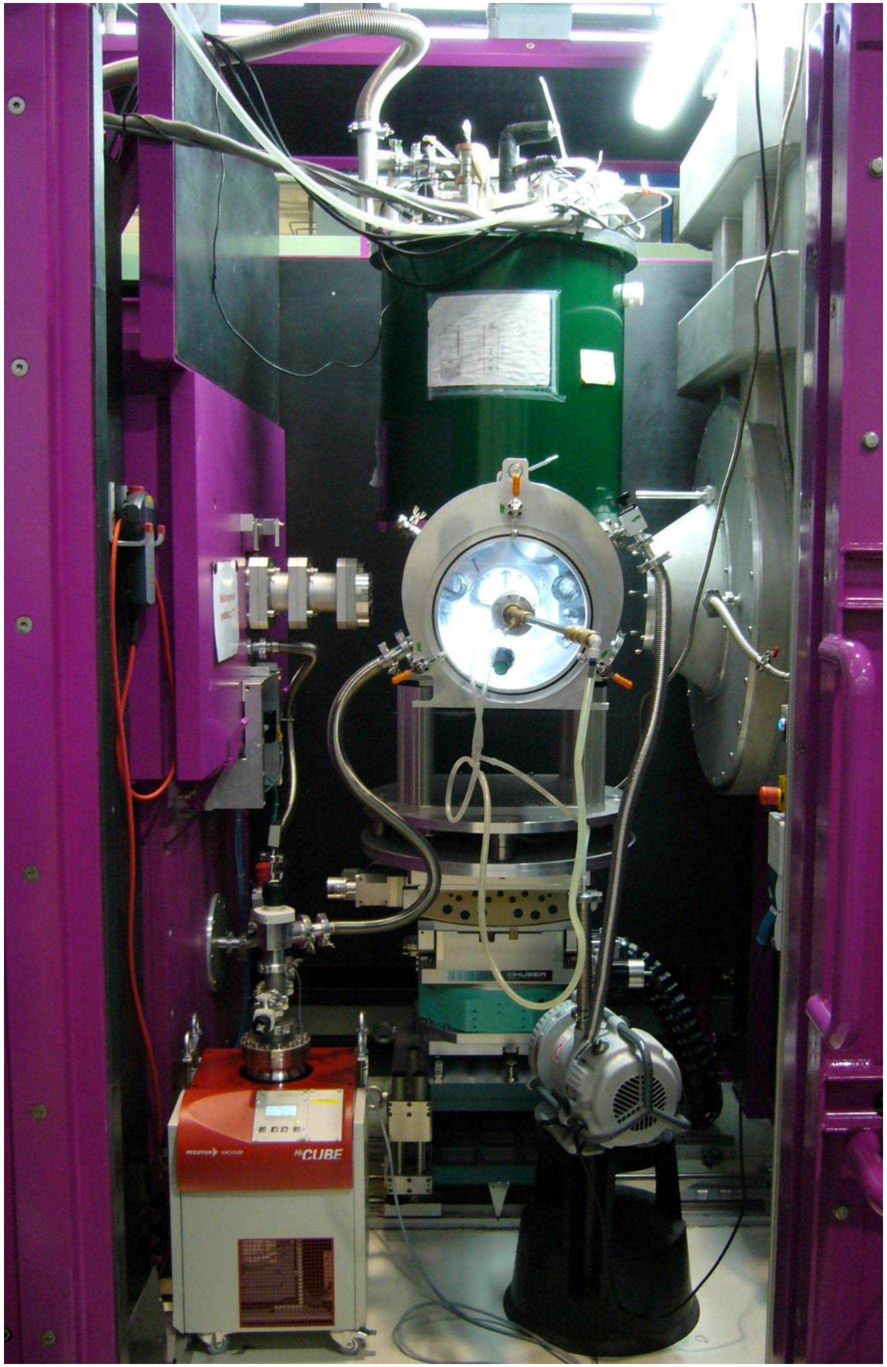

Detector tube

Vacuum vessel for detector to provide lowest possible background

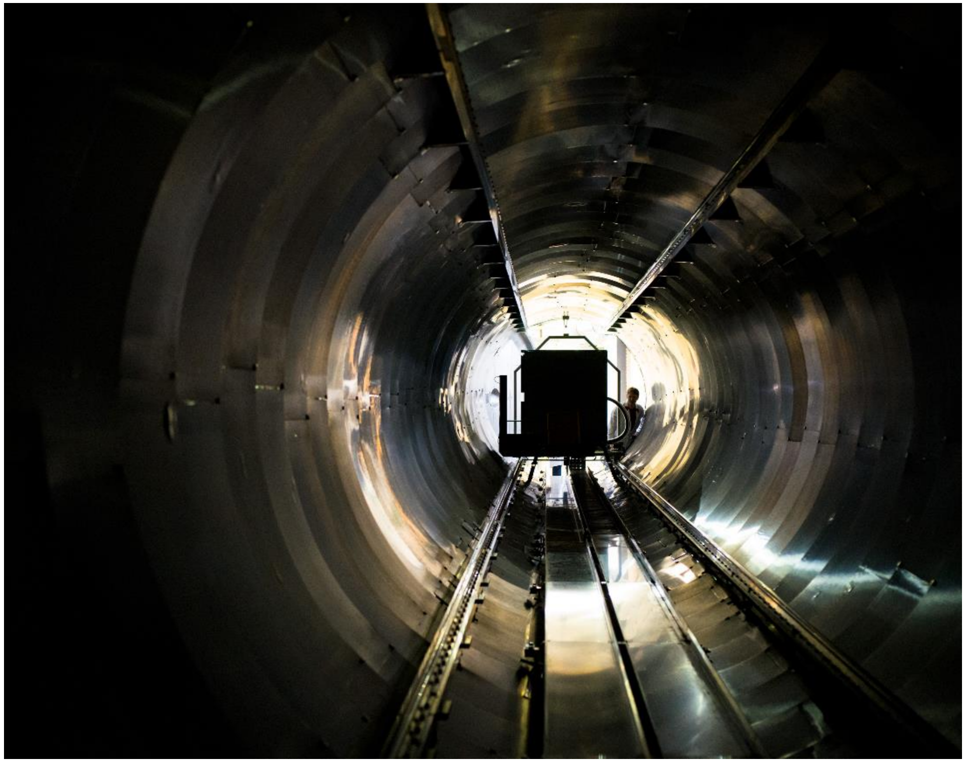

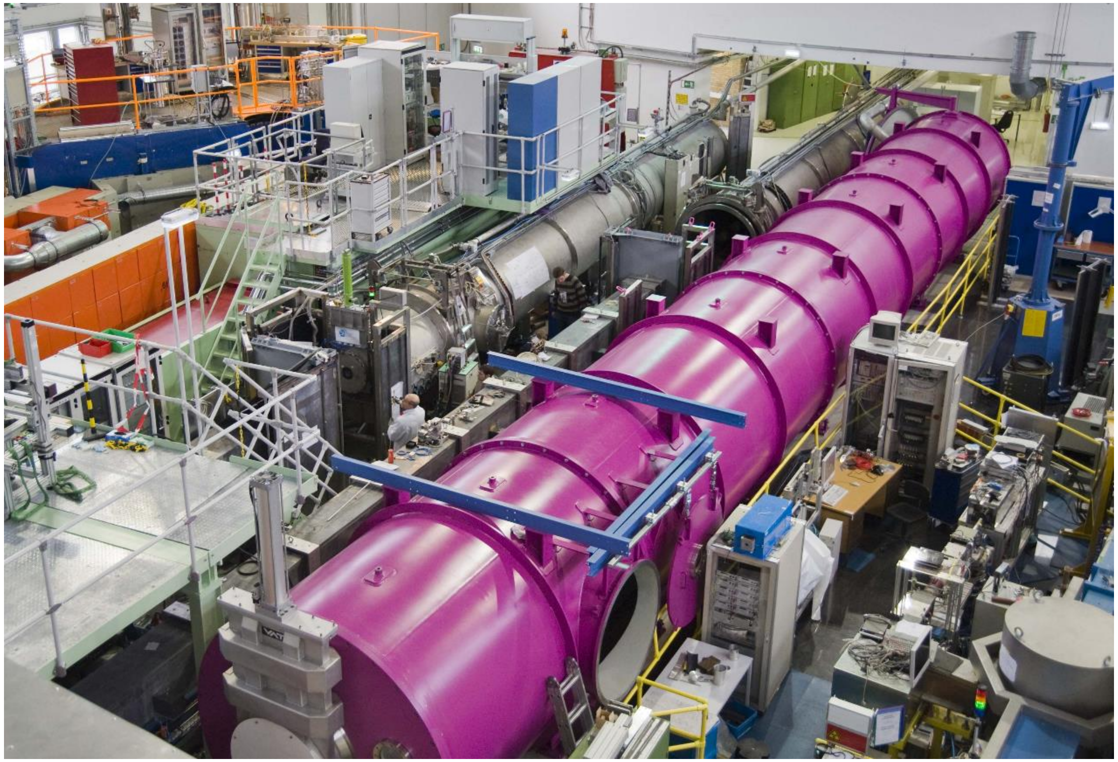

Sample detector length adjustable (select Q-range)

One (or several) He^3 position sensitive detectors (typical $1m^2$ with 5mm resolution)

Typical length 10-40m

Interior completely covered with neutron absorbing Cadmium

Detector

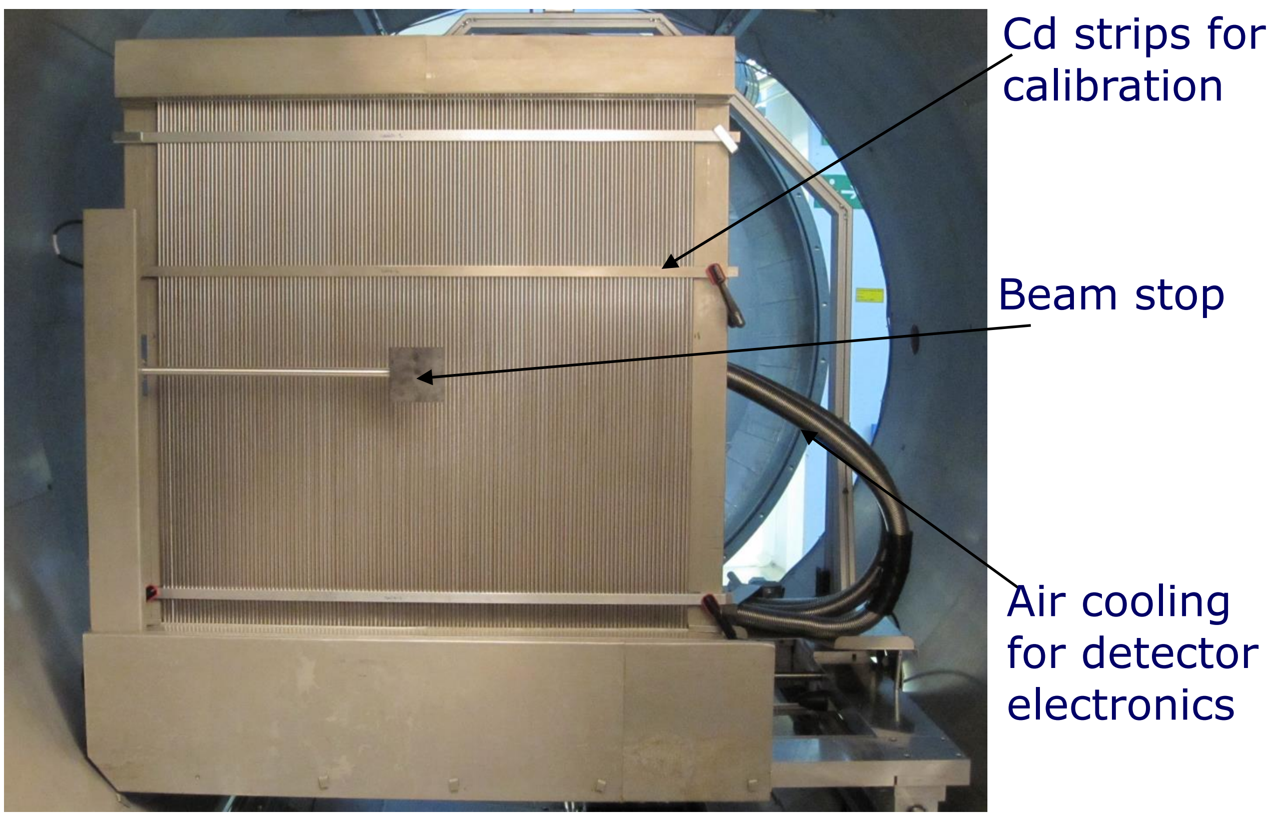

Raw data

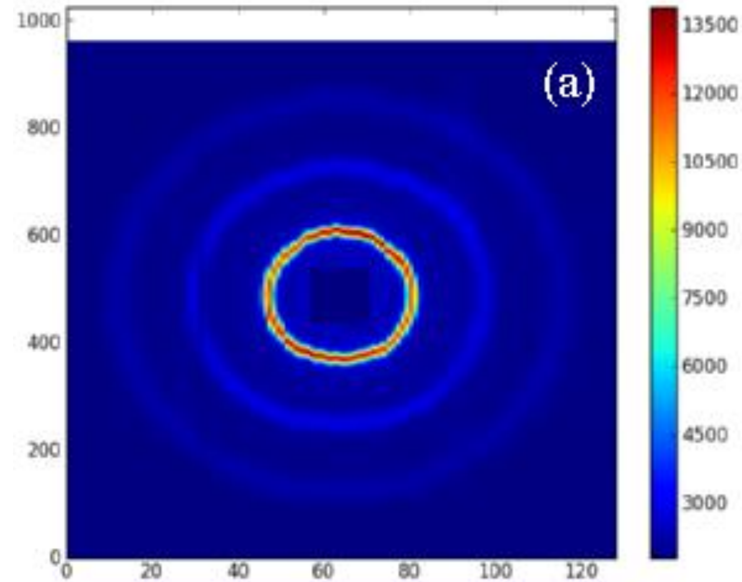

Position calibration

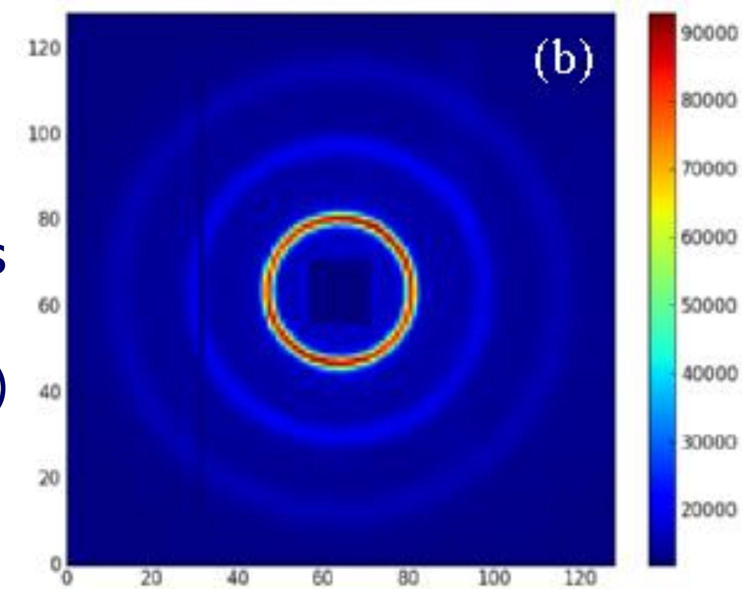

Array of 128 position sensitive ^{3}He Reuter Stokes tube detectors
8mm x 8mm position resolution (charge division)
Detector distance from 1-20m, moves on rails
Maximal count rate 4MHz

SANS – Resolution

$$\frac{\delta\lambda}{\lambda} \approx 0.05 - 0.1$$

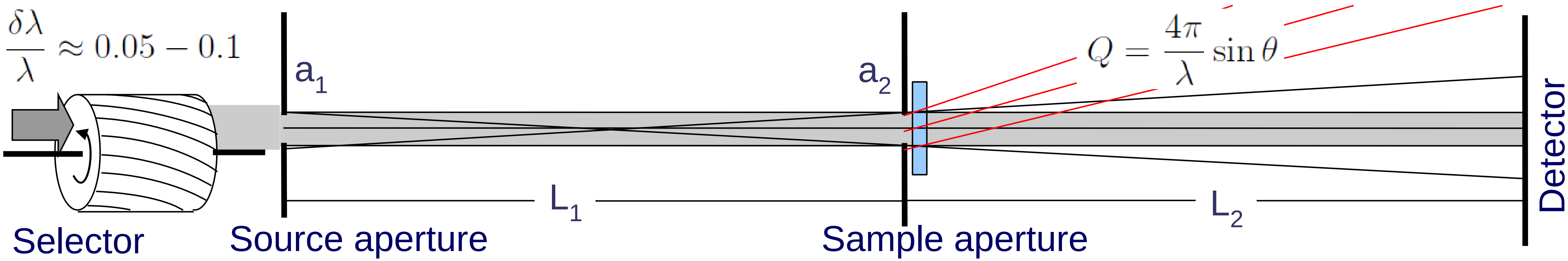

- Angular resolution
- Monochromaicity
- Detector resolution
- Gravity

Treat as Gaussian distributions: $\left\langle \frac{\delta Q^2}{Q^2} \right\rangle = \left\langle \frac{\delta \lambda^2}{\lambda^2} \right\rangle + \left\langle \frac{\cos^2\theta\,\delta\theta^2}{\sin^2\theta} \right\rangle$

$\left\langle \frac{\delta Q^2}{Q^2} \right\rangle = 0.0025 + \left\langle \frac{\delta\theta^2}{\theta^2} \right\rangle$ ⇒ Angular resolution: $\delta\theta \approx \sqrt{\frac{5}{12}\frac{a}{L}}$

What is the largest object SANS can detect (limit small Q)?

For large scattering angles (large Q) wavelength resolution dominates.

For $a_1 = a_2 = a$ and $L_1 = L_2 = L$

⇒ $\delta Q \approx \frac{\delta\theta}{\theta_{min}} Q_{min} \approx \delta\theta \frac{4\pi}{\lambda} \approx \frac{2\pi a}{\lambda L}$

Largest object: $\frac{2\pi}{\delta Q} = \frac{\lambda L}{a}$ On D11, ILL: L=40m, λ=15Å ⇒ D≈ 5μm

SANS – Resolution

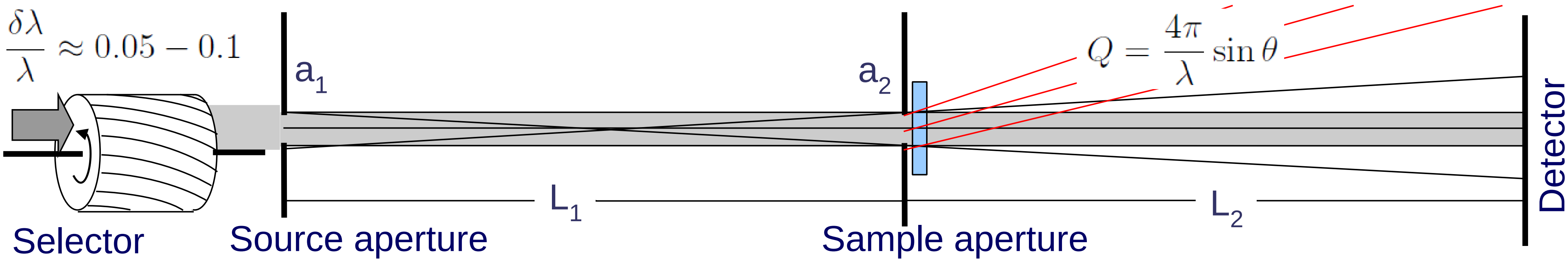

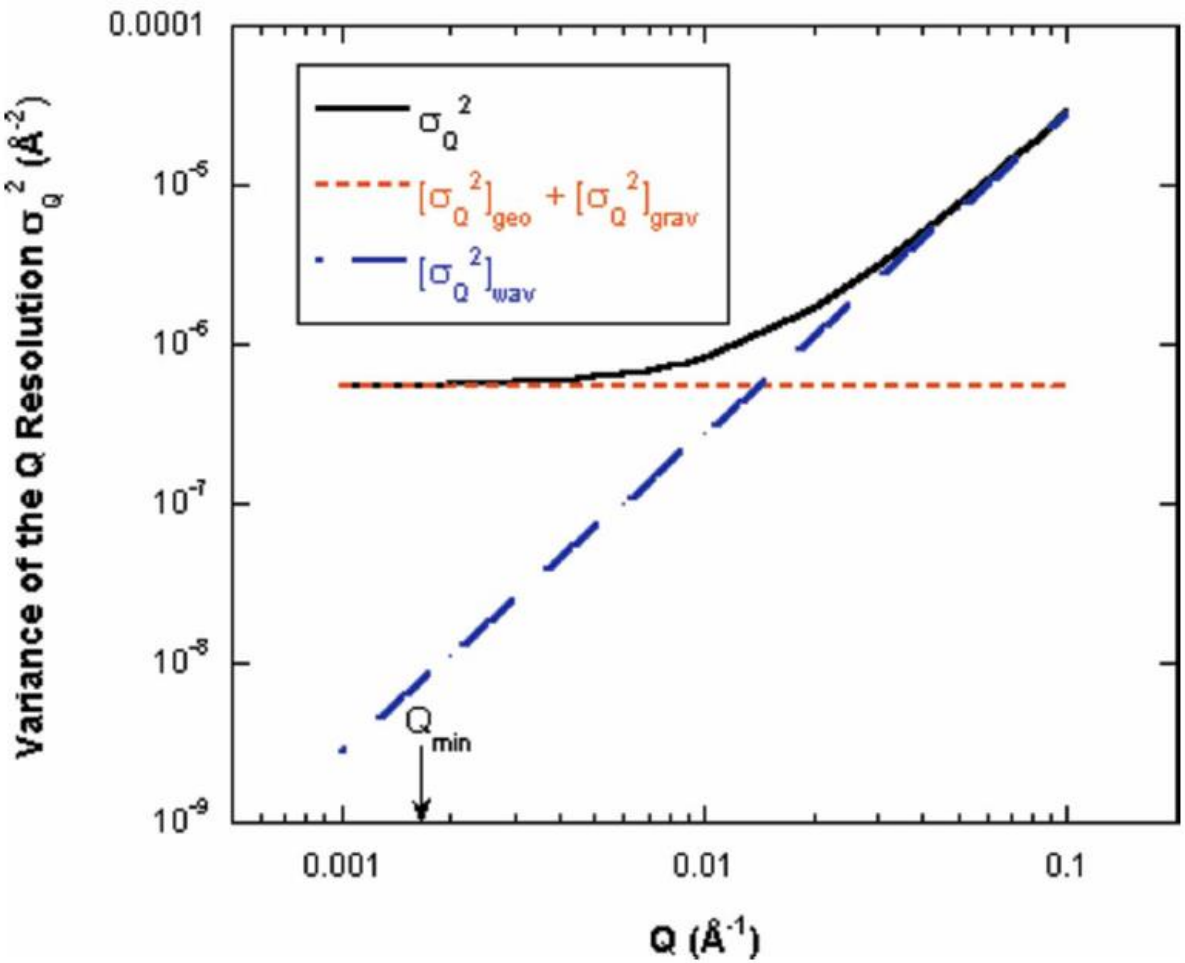

Intensity & Resolution

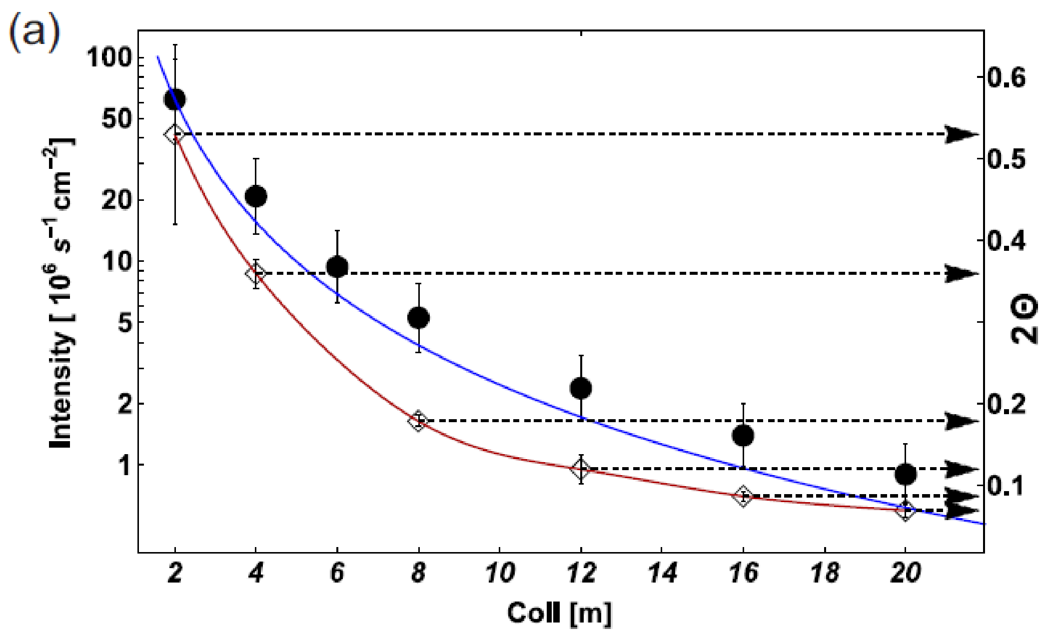

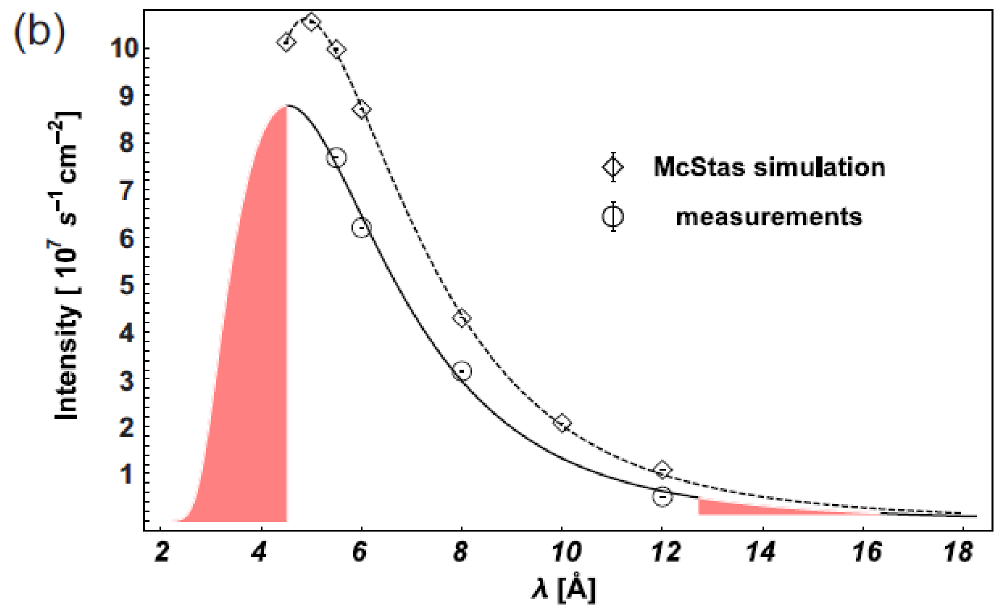

Intensity: Quadratic decrease with source to sample distance (collimation length)

Wavelength: Decrease of intensity with λ^{-4}

$$\delta Q \approx \frac{\delta\theta}{\theta_{min}} Q_{min} \approx \delta\theta \frac{4\pi}{\lambda} \approx \frac{2\pi a}{\lambda L}$$

Typical Measurement

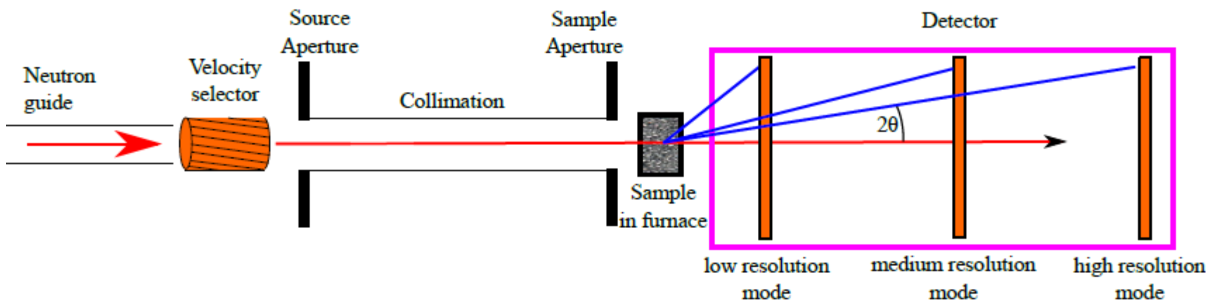

Typical SANS dataset:

- Sample (at different L)
- Water (absolute scale, solid angle correction)
- Empty sample holder/cuvette
- Background (empty beam/blocked beam)

$$\left(\frac{d\Sigma}{d\Omega}\right)_{\text{sample}} = \frac{1}{F_{sc}} \left(\frac{d\Sigma}{d\Omega}\right)^{\text{real}}_{H_2O} \frac{\left[\frac{I_{\text{sample}} - I_{\text{B4C}}}{Tr_{\text{sample}}} - \frac{I_{\text{sample-EC}} - I_{\text{B4C}}}{Tr_{\text{sample-EC}}}\right] \frac{1}{e_{\text{sample}}}}{\left[\frac{I_{H_2O} - I_{\text{B4C}}}{Tr_{H_2O}} - \frac{I_{H_2O\text{-EC}} - I_{\text{B4C}}}{Tr_{H_2O\text{-EC}}}\right] \frac{1}{e_{H_2O}}}$$

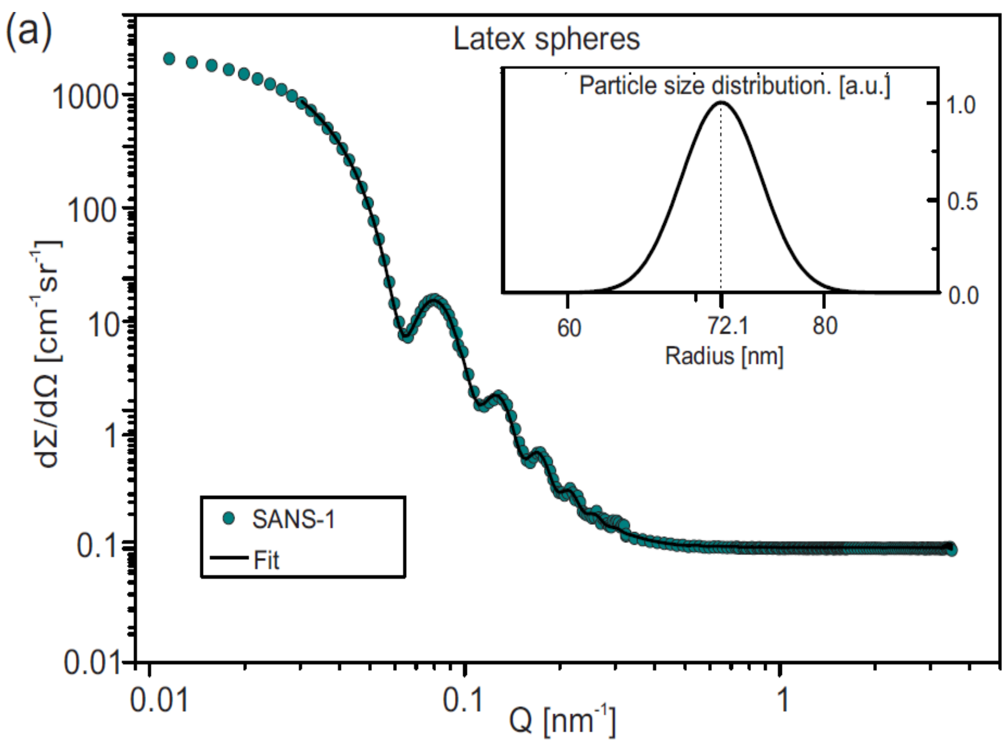

→ Fit model of the sample (conv. with resolution to the dataset)

SANS - Resumee

SANS: Diffractometer specialized for small scattering angles

Large correlations in real space
20 to 40000Å

⟺

Low **Q** small scattering angles
~1 $Å^{-1}$ to ~10^{-4} $Å^{-1}$

SANS tells you the statistical average of:

- Shape of scattering object
- Size (distribution) of scattering objects
- Surface of scattering objects
- Scattering length density (distribution)
- Arrangement (Superstructure?)

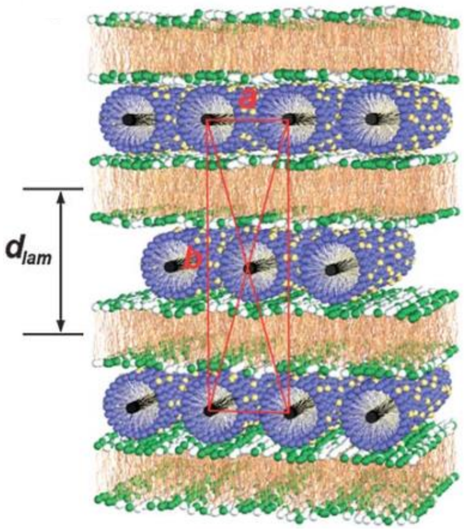

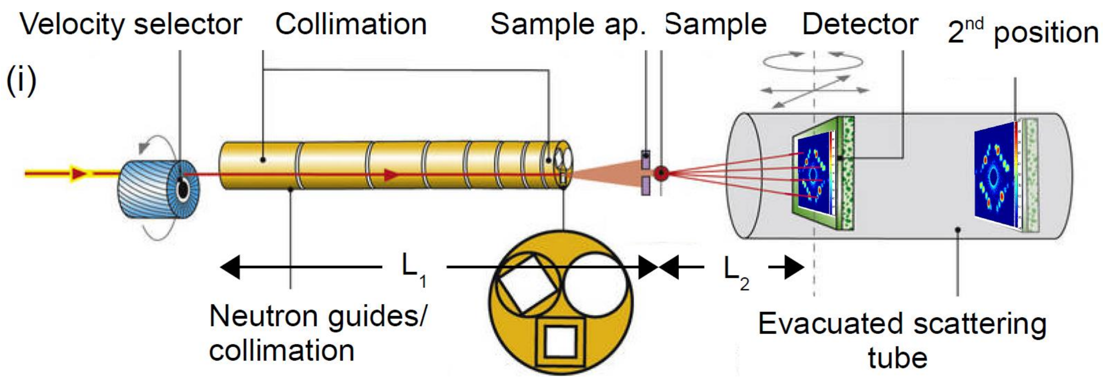

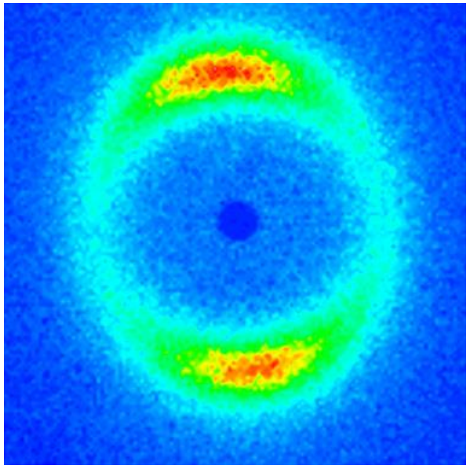

Applications & Examples of SANS:

- Soft Matter
- Hard Matter
- Magnetism of nanoscale materials
- Emergent nanoscale magnetic structures of strongly correlated electron systems

Soft Matter

Polyisoprene – Polystyrene Diblock Copolymer Phase Diagram

Two (or more) homopolymers units linked by covalent bonds
Microphase separation: Complex nanostructures phases

- Flory-Huggins segment-segment interaction
- Degree of polymerization
- Volume fraction

SANS pattern:
Aligned by shear

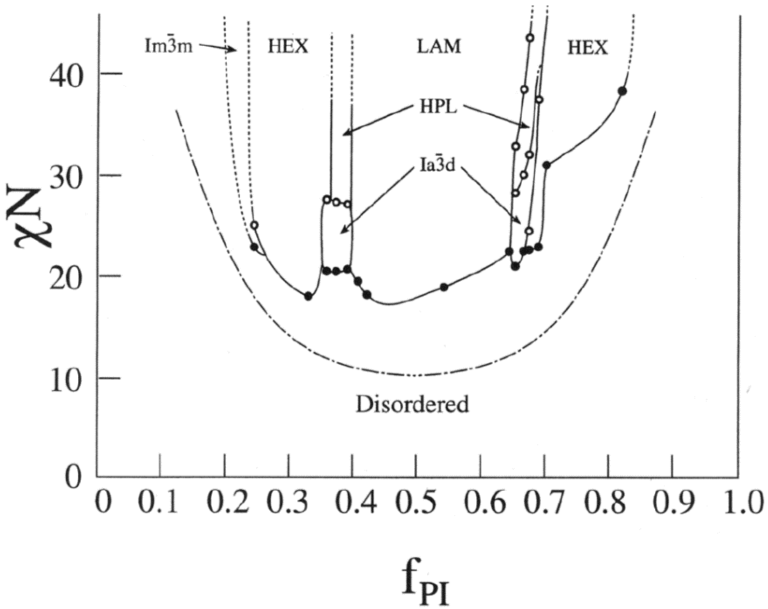

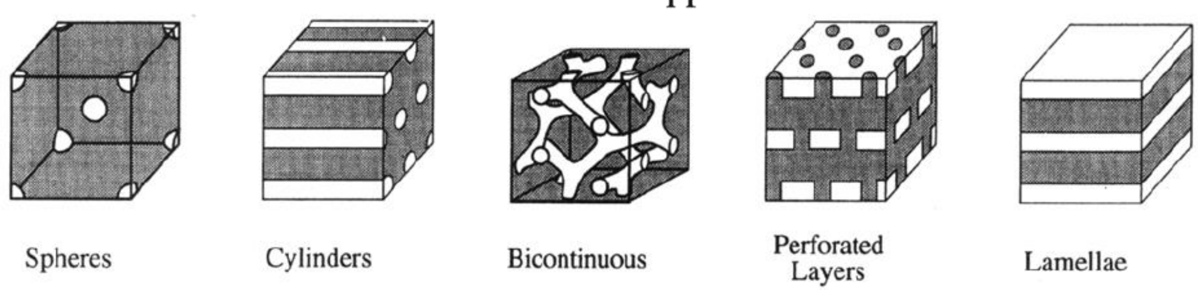

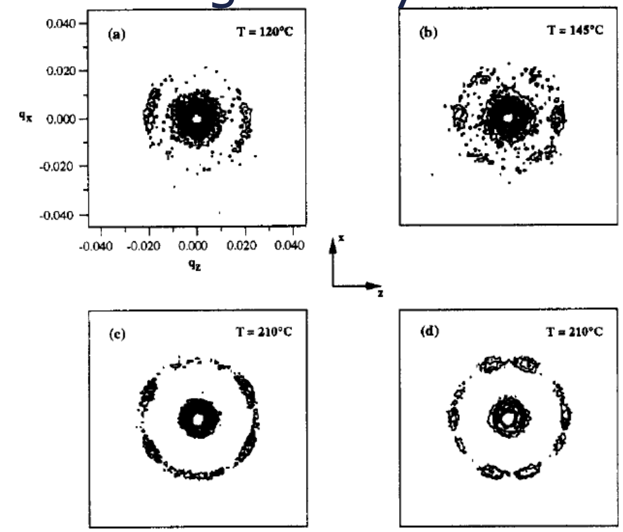

Figure 10. Contour plots of SANS patterns for the sample IS-68 in three different ordered states (A, D, B). A nearly featureless pattern (a) was observed in state A (120 °C), which is attributed to a parallel orientation of lamellae with respect to the shear plane. After heating the sample to 145 °C (state D) and application of dynamic shearing ($\dot{\gamma} = 0.1\ s^{-1}$ with $|\gamma| = 300\%$), a weak hexagonal scattering pattern was observed (b). This is consistent with a hexagonal in-plane arrangement of perforations in the minority (PS) layers. Further heating the sample to 210 °C, without shear (state B), produced a predominantly four-peak pattern (c), which transformed into result (d) when a shear rate of 2.2 s^{-1} was applied. The azimuthal relationship between the combined 10 reflections in (c) and (d) is consistent with the SANS data reported for sample IS-39 (ref 22) and the $Ia\bar{3}d$ space group symmetry.

Macromolecules, Vol. 28, No. 26, (1995)
Physics Today, p. 32, Feb. (1999)

Applications & Examples of SANS:

- Soft Matter
- Hard Matter
- Magnetism of nanoscale materials
- Emergent nanoscale magnetic structures of strongly correlated electron systems

Hard Matter

Co-Re alloys for ultra high temperature / high stress applications (turbine blades) Precipitation growth and ageing by means of SANS.

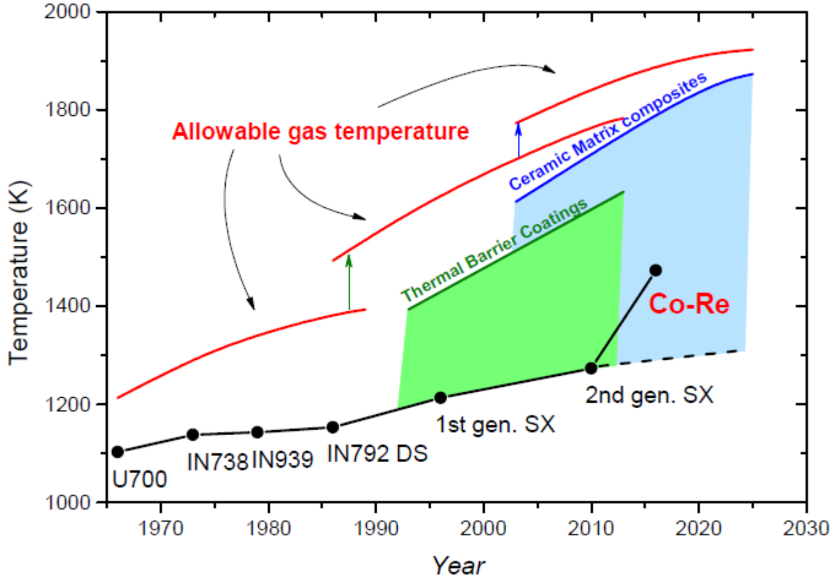

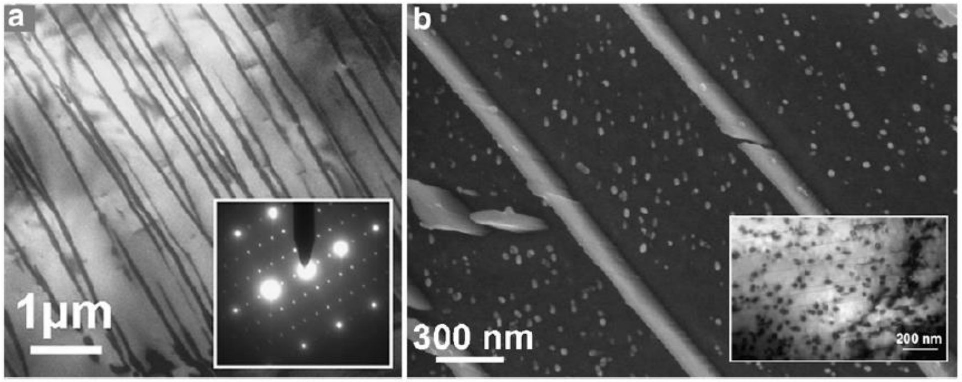

FIGURE 2.1.2: Micrograph from Co-Re-Cr-Ta-C alloy showing various carbide morphologies. (a) The lamellar $Cr_{23}C_6$ type carbides are present with their orientation relationship to the matrix. Inset: Area diffraction pattern. (b) Fine dispersion of TaC, embedded in ϵ-Co matrix, between the $Cr_{23}C_6$ lamellae. The inset shows a TEM image of the TaC precipitates. Adapted from [17]

Precipitation hardening

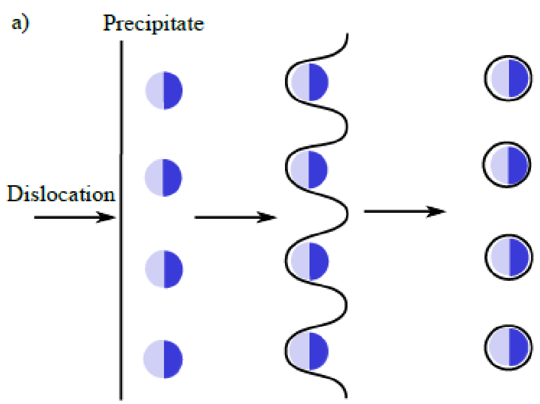

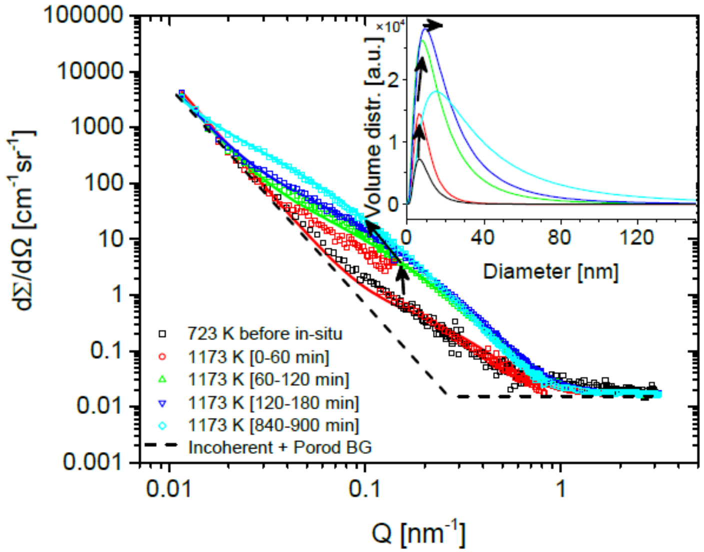

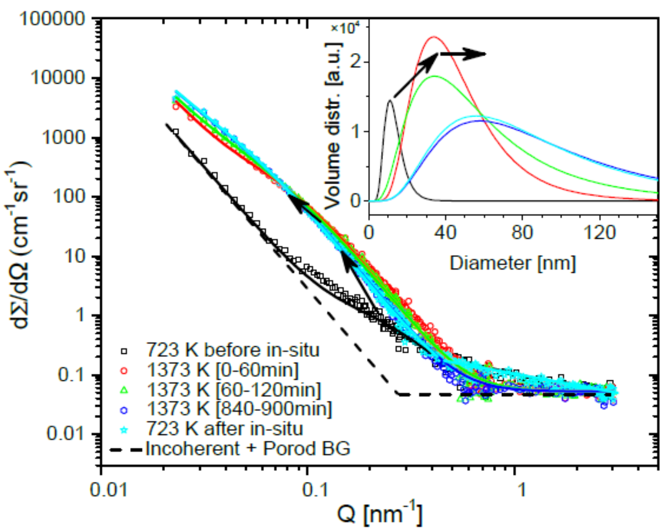

Dissertation L. Karge, TU München

Applications & Examples of SANS:

- Soft Matter
- Hard Matter
- Magnetic SANS
- Magnetism of nanoscale materials
- Emergent nanoscale magnetic structures of strongly correlated electron systems

Magnetic SANS – a primer

Magnetism on the nanoscale (30Å -3000Å)

Magnetism of materials that are inhomogneous on the nanoscale.

Nanoscale magnetism is imprinted by imhomogeneous material/sample properties.

e.g.: Nanoparticles, ferrofluids, sintered NeFeB magnets, granular magnetic recording media, nanodots, magnetic steels….etc

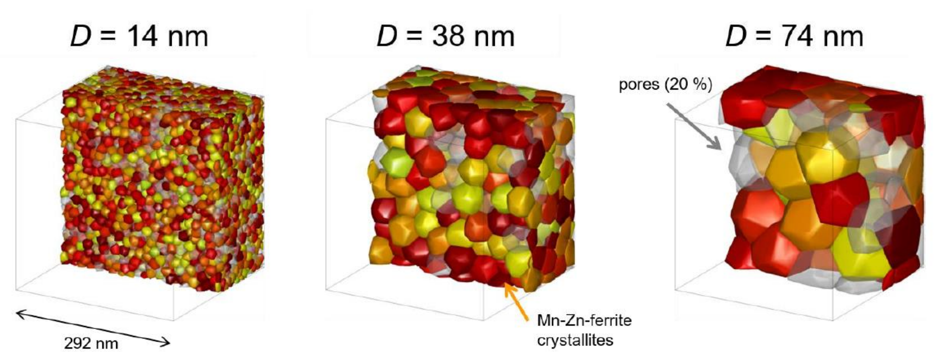

Emergent nanoscale magnetism of spatially homogeneous materials.

Nanoscale magnetism emerges due to (emergent) electronic correlations of SCES, competing interactions or superconductivity

e.g.: Superconducting VL, skyrmions, complex charge / stripe order due to competing FM/AF interactions….

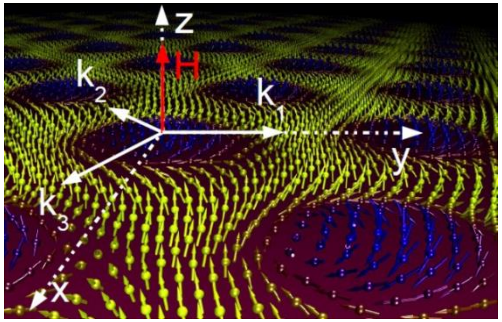

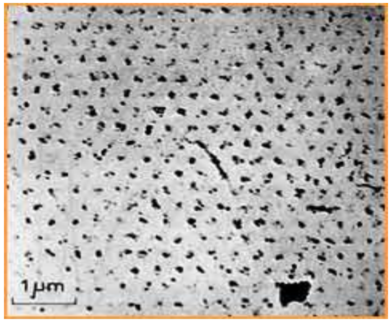

Nanomagnetism

Magnetic SANS is sensitive to the deviation of the mean magnetization:

Nuclear grain microstructure ⇨ Spatial variation of magnetization

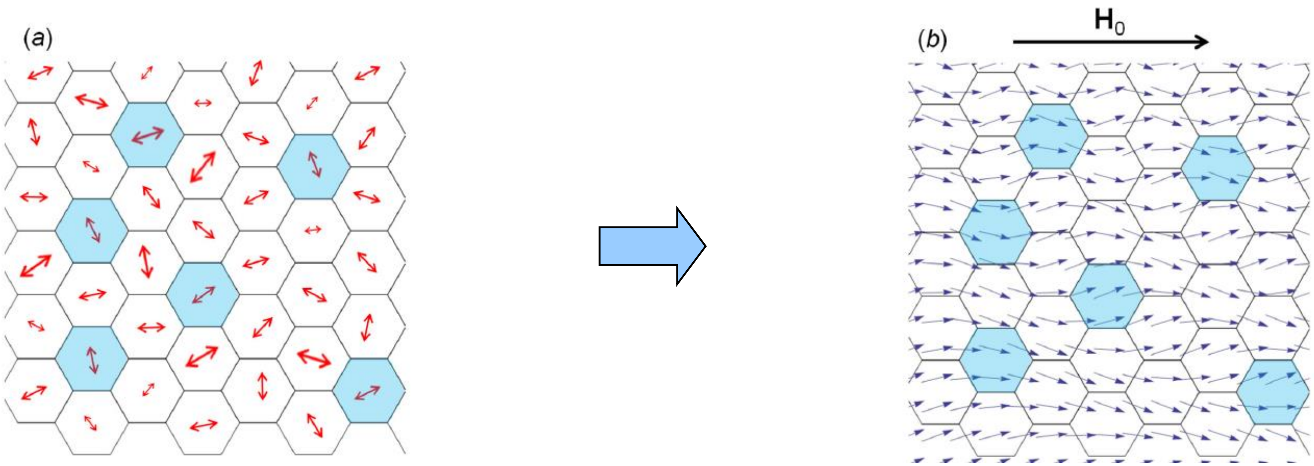

Dissertation D. Mettus, Univ. Luxembourg

⇨ Deviation of the mean spin direction

⇨ Deviation of the mean magnetitude of the magnetization

⇨ SANS: 3D Fourier transform of the magnetization distribution

$$\mathbf{M}(\mathbf{r}) = \{M_x(\mathbf{r}), M_y(\mathbf{r}), M_z(\mathbf{r})\}$$
$$= \frac{1}{(2\pi)^{3/2}} \int_{-\infty}^{+\infty}\int_{-\infty}^{+\infty}\int_{-\infty}^{+\infty} \widetilde{\mathbf{M}}(\mathbf{q})\, e^{i\mathbf{q}\mathbf{r}}\, d^3\mathbf{q}$$

Attention: „Nuclear“ signal in present additionally!

Nanomagnetism

Goal: Relating the microstructure and magnetic properties is of high interest.

Unpolarized magnetic SANS cross-sections

$$\frac{d\Sigma_\perp}{d\Omega} = K\left(b_H^{-2}|\widetilde{N}|^2 + |\widetilde{M}_x|^2 + |\widetilde{M}_y|^2\cos^2\theta + |\widetilde{M}_z|^2\sin^2\theta - CT_{yz}\sin\theta\cos\theta\right)$$

$$\frac{d\Sigma_\parallel}{d\Omega} = K\left(b_H^{-2}|\widetilde{N}|^2 + |\widetilde{M}_x|^2\sin^2\theta + |\widetilde{M}_y|^2\cos^2\theta + |\widetilde{M}_z|^2 - CT_{xy}\sin\theta\cos\theta\right)$$

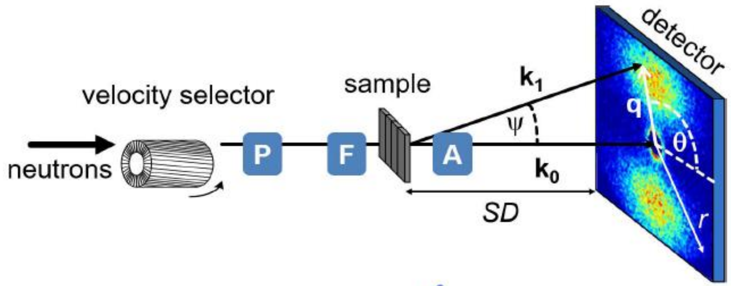

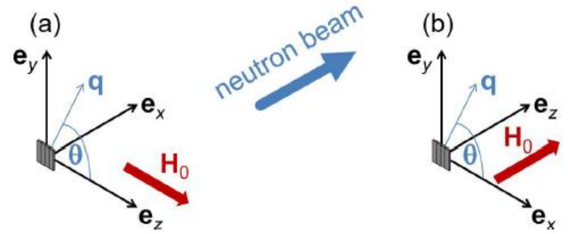

Use magnetic selection rule (anisotropic scattering pattern)

Saturate the sample with high fields to surpress magnetic scattering

Use SANSpol (half polarized) and POLARIS (full polarization analysis) for a full picture/ discrimination of SF/NSF scattering (comes at the price of intensity).

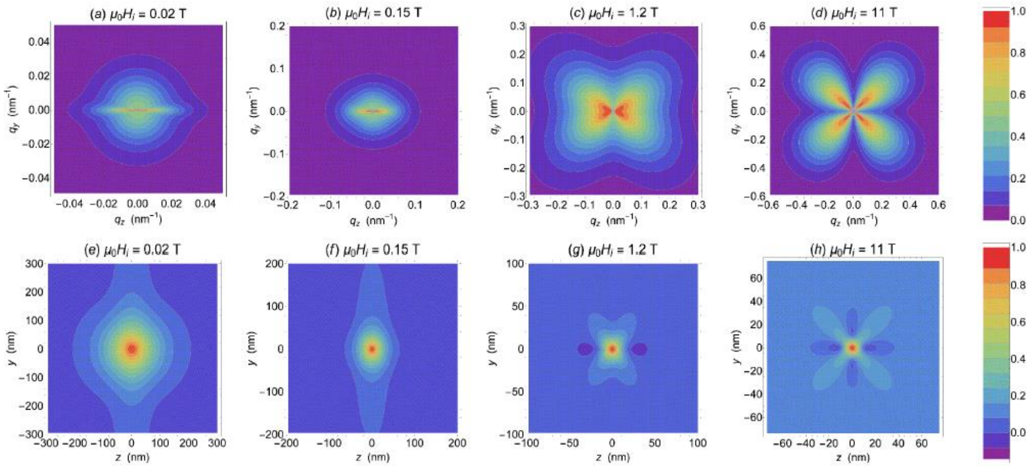

Fig. 2.12 (upper row) (*a*)-(*d*) Contour plots of normalized $d\Sigma_M/d\Omega$ (Eq. (2.58)) at applied magnetic fields as indicated ($\mathbf{k}_0 \perp \mathbf{H}_0$; $H_p/\Delta M = 1$; $\mathbf{H}_0$ is horizontal). For $h^2(qR)$ and $\widetilde{M}_z^2(qR)$, we used the form factor of the sphere with a radius of $R = 5\,\mathrm{nm}$ (Eq. (2.78); $S(q) = 1$). (lower row) (*e*)-(*h*) Corresponding two-dimensional correlation functions $c(y,z)$, which were computed according to Eq. (2.91) ($H_p/\Delta M = 1$).

Incommensurate Magnets

SANS measures inhomogeneities of scattering length density

$$\Rightarrow \frac{d\Sigma}{d\Omega}(\mathbf{q}) = \frac{1}{V}(\rho_1 - \rho_2)^2 \left| \int_{V_1} e^{i\mathbf{q}\cdot\mathbf{r}} d\mathbf{r_1} \right|^2$$

SANS measures mesoscopic information, independent of microscopic structure

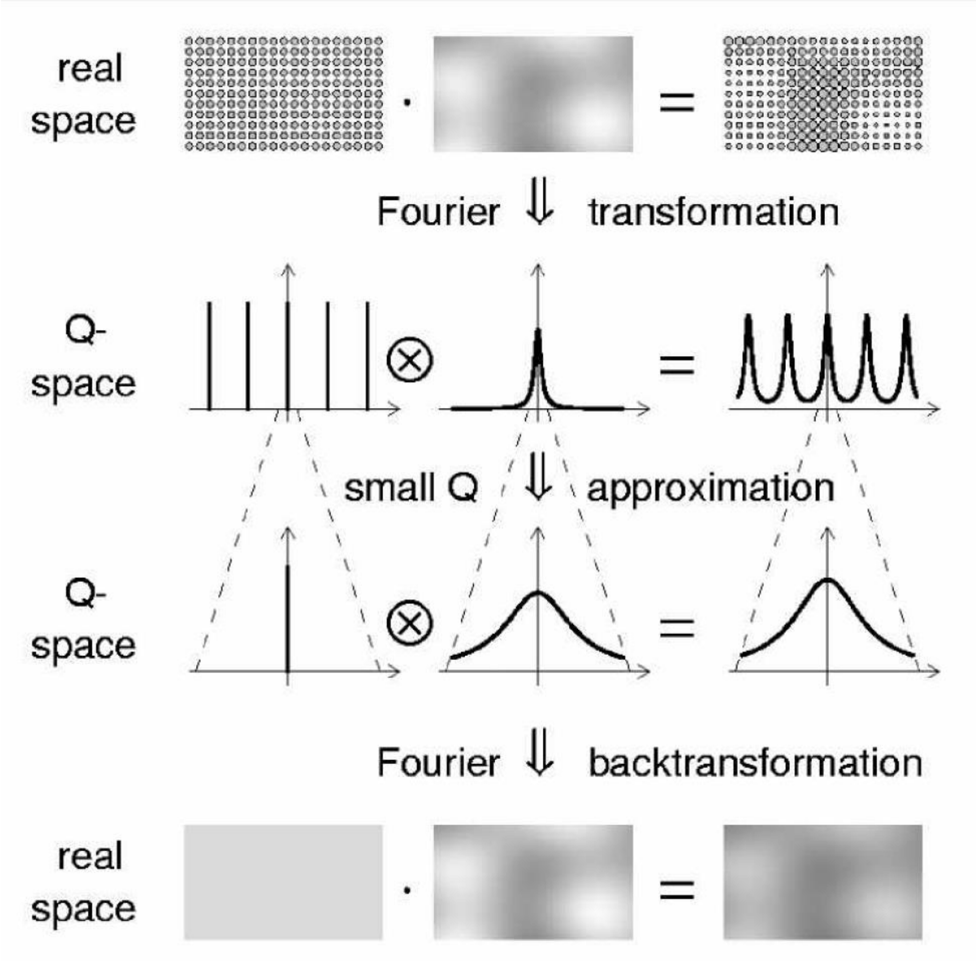

Incommensurate Magnets

Archetypal helimagnet MnSi

Itinerant ferromagnet

No inversion symmetry (B20)
Dzyaloshinsky-Moriya interaction

$H=J(S_1 \cdot S_2)+D \cdot (S_1 x S_2)$

Monochiral helix, pitch=180 Å.

Cubic anisotropy: Weak pinning (111)

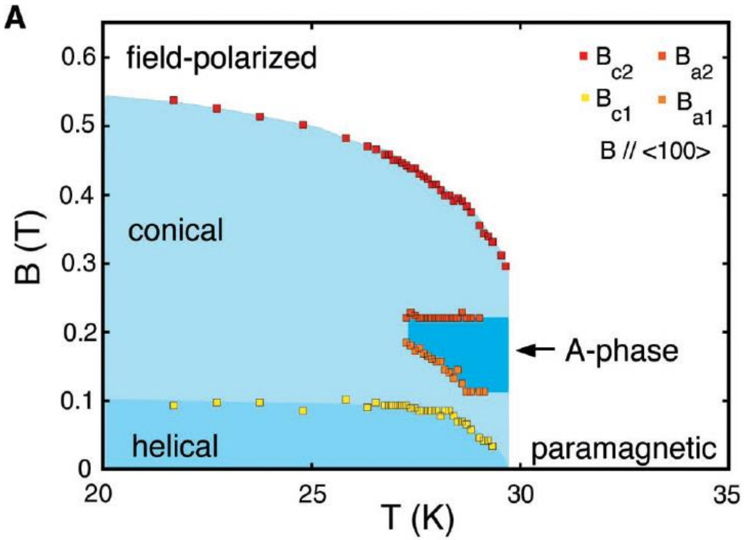

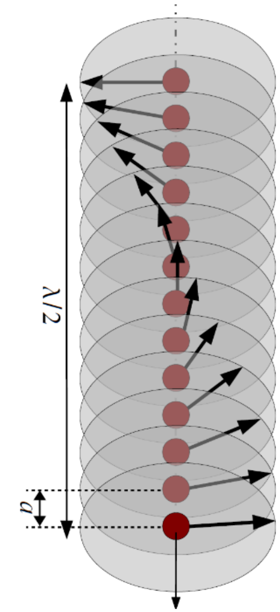

SANS: Incommensurate satellites around (0,0,0)

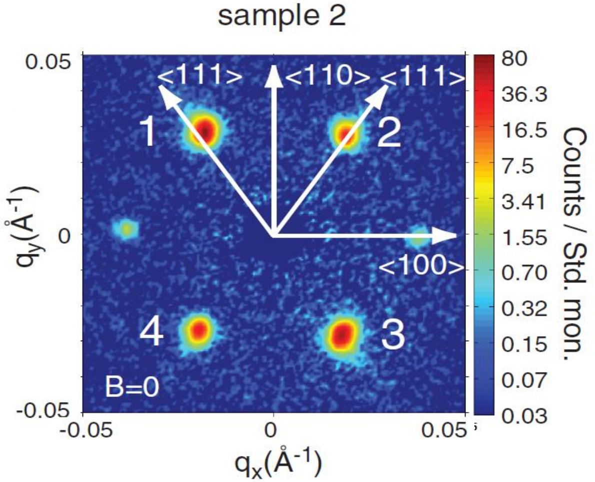

Diffraction: Incommensurate satellites around (h,k,l)

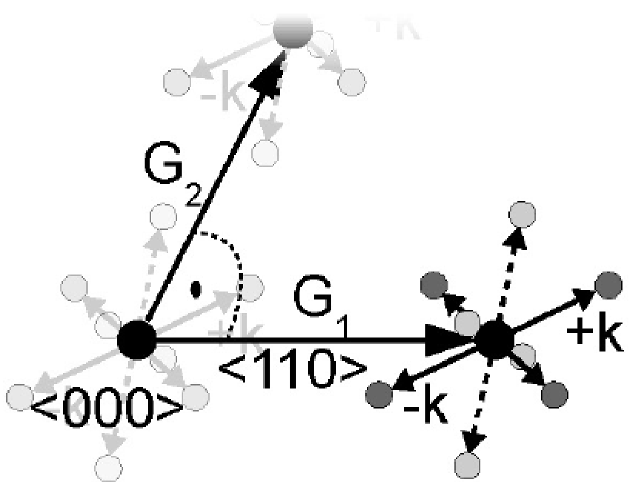

SANS: Vortex Lattices

Vortex lattice crystallography: Diffraction in SANS geometry

Vortex lattice 2D magnetic Bravais lattice

$$\phi_0 = \frac{h}{2e} \qquad |\vec{a}_i| = \left(\frac{2\phi_0}{\sqrt{3}\,B}\right)^{\frac{1}{2}} \qquad |\vec{a}_i| = \frac{2\pi}{|\vec{Q}|}$$

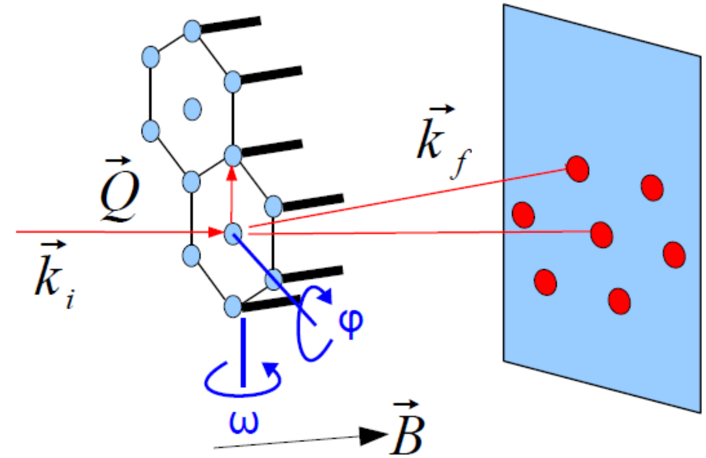

Typical values:

B=1500 G

A_0=1260 Å

Intensity Bragg peak

$$R = \frac{2\pi\gamma^2\lambda_n^2 t}{16\phi_0^2 Q}|h(Q)|^2$$

Form factor

$$h(Q) = \frac{\phi_0}{(2\pi\lambda)^2} e^{\frac{-\pi B}{B_{c2}}}$$

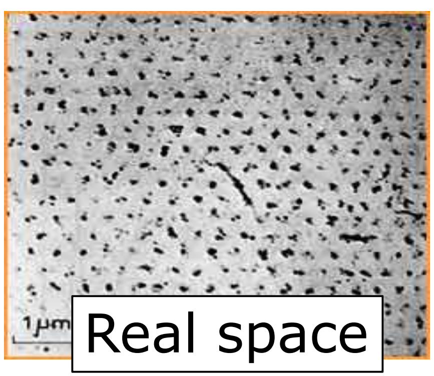

90° rot. around the n-beam

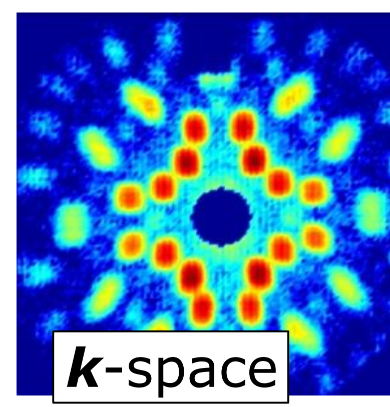

Thank you for your attention!

www.mlz-garching.de
Sebastian.Muehlbauer@frm2.tum.de